

U.S. Geological Survey public-access version of the following article:

Rare earth mineral potential in the southeastern U.S. Coastal Plain from integrated geophysical, geochemical, and geological approaches

By Anjana K. Shah, Carleton R. Bern, Bradley S. Van Gosen, David L. Daniels, William M. Benzel, James R. Budahn, Karl J. Ellefsen, Adam Karst, and Richard Davis

Published in: GSA Bulletin, vol. 129, issue 9-10, May 2017, p. 1140-1157

Any use of trade, firm, or product names is for descriptive purposes only and does not imply endorsement by the U.S. Government

Although this information product, for the most part, is in the public domain, it also may contain copyrighted materials as noted in the text. Permission to reproduce copyrighted items must be secured from the copyright owner.

USGS release date (this version): September 2018

For link to publisher's version, see <https://pubs.er.usgs.gov/publication/70189106>.

1 **Rare-earth mineral potential in the southeastern U.S. Coastal Plain from**
2 **integrated geophysical, geochemical, and geological approaches**

3 A.K. Shah^{1*}, C.R. Bern¹, B.S. Van Gosen², D.L. Daniels³, W.M. Benzel², J.R. Budahn², K.J.
4 Ellefsen¹, A. Karst⁴, and R. Davis⁵

5 ¹*U.S. Geological Survey, DFC MS 964, Box 25046, Denver, CO 80225*

6 ²*U.S. Geological Survey, DFC MS 973, Box 25046, Denver, CO 80225*

7 ³*U.S. Geological Survey, 12201 Sunrise Valley Drive, Reston, VA 20192*

8 ⁴*Iluka Resources, LLC, 12472 St. John Church Rd., Stony Creek, VA 23882*

9 ⁵*Southern Ionics, Inc., 13291 Vantage Way, Ste. 103, Jacksonville, FL 32218*

10 *Corresponding author. Email: ashah@usgs.gov, Phone: 303-236-1218.

11 **ABSTRACT**

12 We combine geophysical, geochemical, mineralogical and geological data to evaluate the
13 regional presence of rare earth element (REE)-bearing minerals in heavy mineral sand deposits
14 of the southeastern U.S. Coastal Plain. We also analyze regional differences in these data to
15 determine probable sedimentary provenance. Analyses of heavy mineral separates covering the
16 region show strong correlations among Th, monazite, and xenotime, suggesting that radiometric
17 equivalent Th (eTh) can be used as a geophysical proxy for those REE-bearing minerals.

18 Airborne radiometric data collected during the National Uranium Resource Evaluation (NURE)
19 program cover the southeastern U.S. with line spacing varying from ~2 to 10 km. These data
20 show eTh highs over Cretaceous and Tertiary Coastal Plain sediments from the Cape Fear arch
21 in North Carolina to eastern Alabama; these highs decrease with distance from the Piedmont.

22 Quaternary sediments along the modern coasts show weaker eTh anomalies except near coast-
23 parallel ridges from South Carolina to northern Florida. Prominent eTh anomalies are also
24 observed over large riverbeds and their floodplains, even north of the Cape Fear arch where
25 surrounding areas are relatively low. These variations were verified using ground geophysical
26 measurements and sample analyses, indicating that radiometric methods are a useful exploration

27 tool at varying scales. Further analyses of heavy mineral separates showed regional differences
28 not only in concentrations of monazite but also of rutile and staurolite, and in magnetic

29 susceptibility. The combined properties suggest the presence of sub-regions where heavy mineral
30 sediments are primarily sourced from either high-grade metamorphic, low-grade metamorphic,
31 or igneous terrains, or represent a mixing of these sources. Comparisons between interpreted
32 sources of heavy mineral sands near the Fall Line and nearby igneous and metamorphic

33 Piedmont and Blue Ridge units showed a strong correspondence with rocks closest to the Fall

34 Line, and poor correspondences with rocks farther inland. This strongly suggests that the primary
35 source of those heavy minerals, especially monazite, is the rocks that formed the rocky coast that
36 was present during Atlantic opening, which in turn indicates the importance of coastal processes
37 in forming heavy mineral sand concentrations. Furthermore, narrow radiometric eTh and K
38 anomalies are associated with major rivers, indicating limited spatial influence of fluvial
39 processes. Later coastal plain sediment deposition appears to have involved reworking of
40 sediments, providing an “inheritance” of the rocky coast composition that persists for some
41 distance from the Fall Line. However, this inheritance is reduced with distance, and sediments
42 within ~100 km of the coast in Georgia and Florida exhibit properties indicative of mixing from
43 multiple sources.

44 INTRODUCTION

45 Rare earth element (REE)-bearing minerals have become increasingly important
46 resources worldwide due to the use of REEs in advanced technology such as cell phones,
47 rechargeable batteries, solar panels, super-magnets, and defense systems. Although REE deposits
48 occur worldwide, more than 95% of global production during the last decade has come from a
49 single country, China (Long et al., 2010; Tse, 2011; Hatch, 2012). In an effort to diversify
50 sources of REE, there is increased interest in evaluating occurrences of REE-mineral
51 concentrations elsewhere. Sediment-hosted deposits are of particular interest because minerals
52 are typically easier to extract than from their igneous and metamorphic counterparts. REE-
53 bearing minerals have been recovered from heavy mineral sand (placer) deposits, typically as
54 monazite [(REEs,Th)PO₄] and xenotime [(REE,Y,U,Th)PO₄], as these minerals are particularly
55 resistant to chemical and mechanical weathering. Monazite has been recovered from placers and
56 stockpiled in Australia, Brazil, India, Malaysia, Sri Lanka, and Thailand (Long et al., 2010;
57 Hoatson et al., 2011; Van Gosen et al., 2014), and is actively being processed for Th and REE's
58 in India (Mohanty, 2015). The development of REE exploration methods and gaining a better
59 understanding of their formation are of high interest.

60 Heavy mineral sand deposits are formed as rivers, streams and coastal processes erode
61 rock and transport sediment to coastal areas where sediments are subsequently deposited and
62 reworked by wind, waves and currents. Sediments become sorted according to density, size,
63 roughness, and shape. Minerals of similar density that are resistant to chemical weathering such
64 as ilmenite, staurolite, rutile, zircon, hematite, and monazite tend to become concentrated
65 together in sands, forming heavy mineral deposits that can be economic. These concentrations
66 typically occur in the form of lenses or layers which, when combined, can be anywhere from a

67 few meters to several kilometers in length and width (Force, 1991; Garnett and Bassett, 2005).
68 Heavy mineral sand deposits are relatively easy to mine where sands are poorly consolidated
69 (usually Cretaceous age or younger) and may provide multiple salable products, such as ilmenite
70 (FeTiO_3), leucoxene (altered ilmenite), rutile (TiO_2), and zircon (ZrSiO_4). Separation methods
71 are typically mechanical, using gravity, magnetic, and less commonly, electrical methods to
72 isolate minerals of interest. Chemical agents are not used in the separation process, and therefore
73 mined areas are relatively easy to remediate (Van Gosen et al., 2014).

74 Economic deposits of heavy mineral sand deposits have been recognized in the
75 southeastern U.S. since the beginning of the 20th century (e.g., Watson and Hess, 1913), and
76 probably earlier (Berquist et al., 2015). The majority of mined deposits are located in Cretaceous
77 and Tertiary sediments near the boundary between the Piedmont and Atlantic Coastal Plain
78 physiographic provinces, commonly referred to as the “Fall Line.” Quaternary sands have also
79 been mined, including the Pleistocene Trail Ridge deposit (Figure 1), and Holocene areas such as
80 at Cove Point, Maryland, and in parts of northeastern Florida (Staatz et al., 1980; Staff, Bureau
81 of Mines, 1987; Berquist et al., 2015). At present, such deposits are typically mined for ilmenite,
82 rutile and zircon. Monazite and xenotime have been recognized as co-minerals (Overstreet, 1967;
83 Staatz et al., 1979; Staatz et al., 1980; Grosz and Schruben, 1994), but concentrations of 1-2% of
84 the heavy mineral assemblage are not currently sufficient for economic recovery. Recent
85 research, however, suggests that monazite concentrations reach up to 12% of the heavy mineral
86 assemblage in some areas, and xenotime concentrations commonly co-vary with monazite, with
87 concentrations up to 1-2% (Bern et al., 2016).

88 Little is understood regarding the provenance of monazite and xenotime in the Atlantic
89 Coastal Plain. The heavy mineral sands have their ultimate sources in the neighboring

90 metamorphic and igneous rocks of the Piedmont and Blue Ridge provinces, but deposit
91 formation is complicated by a >200 m.y. history of erosion and mixing. Early studies (Dryden,
92 1958; Overstreet, 1967) assumed that Coastal Plain monazite was derived from one of several
93 Piedmont monazite “belts” described by Mertie (1953), but neither the delivery mechanism nor
94 the actual source location was determined. More recent provenance studies have focused on
95 fluvial inputs at the local scale (e.g., Darby, 1984; Naeser et al., 2006) and reveal little about
96 monazite or xenotime. Literature describing studies of detrital zircon and detrital monazite from
97 Atlantic Coastal Plain sediments is currently very sparse.

98 Radiometric methods provide an approach for exploration and characterization of heavy
99 mineral sand deposits, particularly those containing REE-bearing minerals (e.g. Meleik et al.,
100 1978; Mudge and Teakle, 2003; Singh et al., 2007). Natural gamma photons emitted during
101 radioactive decay series of potassium (K-40), thorium (Th-232), and uranium (U-238 and U-235)
102 isotopes (e.g., Force et al., 1982) are measured; spectral properties may be used to estimate
103 relative amounts of K, U and Th. Many early airborne radiometric surveys in the southeastern
104 U.S. measured only gamma total count because they were conducted before spectral methods
105 were fully developed. Total count highs over Atlantic Coastal Plain sediments have been
106 associated with both U in phosphates and Th in heavy mineral sands (Force et al., 1982; Grosz,
107 1983; Grosz et al., 1989). Some of these observations were later verified with ground or airborne
108 spectral data showing relative contributions of K, U, and Th (Grosz et al., 1989; Grosz et al.,
109 1992). In the Piedmont, total count highs have been observed over high-grade metamorphic
110 rocks, presumably due to monazite, but also over felsic igneous rocks containing potassium
111 feldspars (Pitkin, 1968; Neathery et al., 1976).

112 Magnetic methods have also been used to explore for placer deposits. The success of
113 these methods depends on the presence of magnetic minerals (e.g. magnetite, maghemite,
114 hematite and to a lesser degree ilmenite) within the heavy mineral assemblage, and percentage of
115 these minerals within the bulk sand being high enough so that a detectable anomaly is generated.
116 Early efforts to use aeromagnetic surveys were typically not successful (Wynn et al., 1985),
117 although more recent low-altitude (<50 m) airborne surveys have shown anomalies associated
118 with heavy mineral concentrations in South Australia (Mudge and Teakle, 2003). Greater success
119 has been attained using ground and shipboard surveys, attributable to the reduced distance
120 between source and sensor (Siddiquie et al., 1984, Peterson et al., 1986; Shah et al., 2012; Shah
121 and Harris, 2012). The use of magnetic methods in placer deposit exploration is described in
122 further detail by Van Gosen et al. (2014).

123 We have combined airborne and ground geophysical data with geochemical and
124 mineralogical studies of sand samples to delineate concentrations of the REE-bearing minerals
125 monazite and xenotime at the regional scale across the southeastern U.S. Coastal Plain. These
126 data reveal broad, regional variations in the heavy mineral assemblages that have implications
127 for source rock type. Further analyses show how heavy mineral concentrations may be broadly
128 traced to their sources in the Piedmont and Blue Ridge provinces, providing insights into the
129 dominant processes forming these deposits. These variations also show a regional dependence
130 for the sensitivity of geophysical methods from which we suggest corresponding exploration
131 strategies.

132 **GEOLOGIC SETTING**

133 The Atlantic Coastal Plain, consisting of sediments and sedimentary rocks of Jurassic to
134 Holocene age, first formed with the opening of the Atlantic Ocean. With opening, erosion of the

135 ancient metamorphic and igneous coastline by coastal processes and fluvial transport from inland
136 areas brought sediments to the new coast. Once delivered and deposited, those sediments
137 continued to be reworked by waves, currents, and winds until buried by subsequent deposition.
138 The original rocky coastline is visible today as steep topographic gradients along the boundary
139 between the Coastal Plain and Piedmont provinces. This boundary is commonly referred to as
140 the “Fall Line,” partly for associated waterfalls such as Great Falls, Va., and Roanoke Rapids,
141 N.C. As the Atlantic Coastal Plain grew, sediments continued to be reworked and mixed by both
142 coastal and fluvial processes. Relics of changes in sea level and deposition can be observed in
143 various features such as topographic ridges and barrier islands parallel to the coast.

144 The system of rises and embayments in bedrock along the coastline of the eastern U.S.
145 has likely influenced transport of coastal plain sediments at the regional scale and the resulting
146 shape of the modern shoreline (Owens and Gohn, 1985). Prominent rises include the Cape Fear
147 arch in North Carolina and the Peninsular arch in Florida (Figure 1). The rises would have
148 blocked longshore transport and thus potential mixing from different areas. They also locally
149 inhibited deposition of marine and terrigenous sediments. For example, surface sediments over
150 the Cape Fear arch are Cretaceous in age, while surrounding sediments are Paleogene or younger
151 (Figure 1).

152 The metamorphic and igneous Piedmont and Blue Ridge provinces serve as the primary
153 source for heavy mineral sands within the Atlantic Coastal Plain (Force, 1991). The Piedmont
154 and Blue Ridge have experienced multiple episodes of compression and extension and display a
155 diverse array of rock types of varying age. However, even though these provinces are very
156 complex, various workers have recognized regions commonly referred to as “belts” that reflect
157 different episodes of metamorphism and intrusive emplacement (e.g., Hatcher and Odum, 1980).

158 These include the Carolina and Eastern slate belts, which are marked by slate and other low-
159 grade metamorphic rocks as well as intrusive rocks; the Raleigh/Goochland belt, the Kiokee and
160 Uchee belts, and the Inner Piedmont, which are marked by high-grade metamorphism; and the
161 Charlotte belt, which contains numerous granitoid intrusions (Figure 2).

162 The presence of monazite in the Piedmont is well documented. Through analyses of
163 stream sediments, Mertie (1953, 1979) proposed the existence of three monazite belts that
164 extended much of the length of the Piedmont and Blue Ridge (Figures 1-2). Comparisons to
165 surrounding geologic units demonstrated that large sections of the monazite belts overlap areas
166 of high-grade metamorphism, leading Overstreet (1967) to propose a metamorphic source for
167 Piedmont monazite. However, monazite has also been observed within granitoid intrusions such
168 as the Liberty Hill pluton in South Carolina, and in some cases, the monazite belts include both
169 intrusive and metamorphic rocks.

170 **METHODS AND MATERIALS**

171 **Airborne geophysical data**

172 During the 1970s, as part of the National Uranium Resources Evaluation (NURE)
173 program, airborne radiometric and magnetic surveys were conducted over most of the
174 conterminous U.S. In order to cover such a large area, the line spacing of these surveys typically
175 varied from 5-8 km. The resolution of these data is thus very coarse, but they remain one of the
176 few datasets covering most of the southeastern U.S. The spectral properties of measured gamma
177 emissions were processed in order to estimate relative values of K, U, and Th; surveys were
178 leveled relative to each other in order to provide continuous data at a national scale (Duval et al.,
179 2005). Because multiple gamma emission events are associated with both the U and Th decay
180 series, each with different corresponding energy spectra, estimates are usually referred to as

181 equivalent U and Th (eU and eTh, respectively). We note that gamma emissions generally reflect
182 rock and sediment within about 0-100 cm of the surface because gamma photons from the decay
183 of deeper sources tend to be scattered (through Compton scattering) before reaching the
184 atmosphere and thus the sensor. However, in many cases the gamma particles are emitted from
185 residual soils derived from deeper underlying rock or sediments. Areas covered with water
186 usually produce no gamma emissions due to impenetrability.

187 During the 1960s and 1970s, a number of aeromagnetic surveys with 1.6-3.2-km line
188 spacing and 120-150 m height above ground were flown in the southeastern U.S. Total count
189 scintillometer sensors were added to many of these surveys although the technology was still
190 emerging and standards had not been established. In South Carolina, a combination of six such
191 surveys produced total count data for about 90% of the state with 1.6 km (1-mile) line spacing.
192 Using total count data from two NURE 4.8-km (3-mile) surveys to fill the remaining 10%, we
193 leveled the survey data relative to each other to create a statewide map. The total count data do
194 not distinguish among K, U and Th sources, but the closer flight line spacing provides intensity
195 information at a much more detailed scale than the NURE surveys.

196 Airborne magnetic data are available at the national scale through the Magnetic Anomaly
197 Map of North America (North American Magnetic Anomaly Group, 2002). These data were later
198 corrected for long wavelength variations (Ravat et al., 2009). In the Piedmont and Blue Ridge
199 provinces, numerous workers have explored correspondences between magnetic anomalies and
200 surface or subsurface rocks (e.g., Hatcher and Zietz, 1980); these maps thus complement
201 radiometric survey data. In the Atlantic Coastal Plain, magnetic survey anomalies generally
202 reflect buried basement rock. The distance between sensor and source combined with relatively

203 coarse sampling along flight lines makes detecting sedimentary sources very challenging (e.g.,
204 Shah et al., 2012).

205 **Regional sample measurements**

206 Geophysical measurements of heavy mineral sands reflect the combined effect of the
207 concentration of heavy minerals within the sands and the composition of the heavy mineral
208 assemblage. This creates ambiguity in interpretation: for example, a Th anomaly may represent a
209 minor concentration of heavy minerals that is rich in monazite, or it may represent a rich
210 concentration of heavy minerals with only a small component of monazite. Analyses of heavy
211 mineral separates, i.e., samples that include sands of a minimum density (typically 3.3 g/cm³),
212 allow distinction between the two scenarios. In particular, regional differences in heavy mineral
213 separate mineralogy can allow “calibration” of geophysical anomalies by indicating whether
214 heavy mineral concentrates are likely to be rich in Th-bearing minerals, magnetic minerals, or
215 both. Mineralogy may also provide information regarding source rock if linkages to igneous
216 and/or metamorphic mineralogy can be made. It is important to note that sorting of sands as they
217 are reworked will also create local variations that can make such linkages less clear.

218 We conducted laboratory measurements of magnetic susceptibility and radioactivity of
219 heavy mineral separates derived from sand samples collected at field sites (Figure 1).
220 Concentrations of 55 elements were measured on heavy mineral separates by SGS Mineral
221 Services using inductively coupled plasma atomic emission spectroscopy and mass-spectrometry
222 (ICP-AES-MS) after decomposition of the sample by a sodium peroxide sinter. X-ray diffraction
223 (XRD) was used to estimate mineral content of the separates. In order to increase regional
224 coverage, geophysical and geochemical properties of a subset of archived stream sediment
225 samples collected during the NURE program (Smith, 1997) were also measured. The NURE

226 samples were chosen with a slight bias, where those samples showing greater concentrations of
227 La were favored to assist studies of REE minerals. Samples were also collected from ground
228 survey sites where a significant fraction of heavy mineral sands could be extracted, as is
229 discussed below. The geochemical and XRD data are described in detail by Bern et al. (2016).

230 **Ground geophysical surveys**

231 The NURE and total count airborne surveys provide coverage over large areas, but they
232 reveal little information regarding the distribution of source materials at a local scale.

233 Furthermore, radiometric and magnetic anomalies can arise from a number of different types of
234 geological sources. In order to ground-truth the airborne data, we conducted ground surveys
235 using a portable gamma spectrometer (a Radiation Solutions RS-125 and a GF Instruments
236 Gamma Surveyor) and handheld cesium magnetometer (a Geometrics G-858 gradiometer
237 system). The surveys took place between February 2013 and March 2015.

238 The survey sites, shown in Figure 1, were chosen based on (1) the presence of airborne
239 NURE Th and/or total count anomalies, (2) whether the local surface geology suggested heavy
240 mineral sand potential (3) coverage of diverse ages, (4) a wide geographic distribution, (5)
241 accessibility of sites, and (6) in some cases, availability of drill hole data. The sites included
242 Cretaceous sands (Cheraw State Park, South Carolina and Aurelian Springs, North Carolina; the
243 latter represent terrace deposits), Pleistocene sand bars (near the Folkston deposit in southeastern
244 Georgia), Holocene fluvial floodplains in eastern South Carolina and southern Virginia (Frances
245 Marion State Forest and the James River), and modern coastal sites from North Carolina to
246 Florida (the Outer Banks, Folly Beach, Cumberland Island and Little Talbot Island).

247 Where feasible, surveys were conducted along profiles spaced 50-200 m apart, usually in
248 a “mow-the-lawn” configuration. At some sites, accessible areas were narrow due to dense forest

249 or sand dunes, so data in these instances were collected along a single profile. Some areas were
250 relatively small so only a few assay measurements were taken. For continuous measurement
251 recordings along profiles, the RS-125 calculates a running average of total count readings while
252 the Gamma Surveyor averages spectral readings over a fixed time period (for this study, 30
253 seconds). To verify contributions to RS-125 total count data, specific sites were also occupied for
254 1 minute or more, allowing for a spectral calculation. During the surveys, either the RS-125 or
255 the Gamma Surveyor was available, but not both. A subset of sites was thus reoccupied using
256 both instruments to estimate consistency between the different meters. For sites that were re-
257 occupied within 4 m of each other, the difference in eTh measurements was less than 5% of the
258 larger value, while for sites within 10 m of each other the differences were less than 35%. The
259 difference in radiometric K and eU varied more widely, probably because both of these values
260 were very low and close to the detection limits of the instrument. A summary of these data is
261 provided in the GSA Data Repository.

262 Where the width of the survey area allowed, tie-line profiles were used to level magnetic
263 survey data. At sites where tie lines could not be obtained, survey data were leveled relative to
264 regional airborne magnetic grids (Ravat et al., 2009). In order to highlight shallow magnetic
265 sources (within a few dozen meters from the surface), profiles were upward continued a distance
266 of 50 m, and the upward continued profile was subtracted from the observed profile. All survey
267 data were corrected for diurnal variations through the use of a magnetic base station set up near
268 the survey site.

269 Samples were collected at field sites. In beach areas, grab samples were obtained with
270 spacing 50-500 m, depending on the size of the survey area. In soil-covered areas, samples were
271 collected by hand auger. For these samples, either a Niton XL3t GOLDD+ portable X-ray

272 fluorescence (XRF) analyzer or ICP-AES-MS was used to estimate chemical concentrations. A
273 ZH Instruments SM-30 was used to estimate magnetic susceptibility. Two of the ground survey
274 sites, near Aurelian Springs, North Carolina, and north of Folkston, Georgia (the “Mission”
275 mine) are actively being explored for ilmenite, zircon, and other heavy minerals by Iluka
276 Resources, Inc. and Southern Ionics, Inc., respectively. In Aurelian Springs, Iluka drilled various
277 sites and obtained measurements of heavy mineral content and major element geochemistry.
278 Southern Ionics, Inc. acquired similar data for the Mission mine.

279 **RESULTS**

280 **Regional airborne geophysical data**

281 Correlations between sample Th and La (Grosz, 1993) and among Th, monazite, and
282 xenotime (Bern et al., 2016) have been observed throughout the southeastern U.S., indicating a
283 direct link between Th and REE-bearing minerals. Radiometric equivalent Th (eTh) is thus of
284 primary interest. Radiometric K is also of interest because it tends to reflect the presence of K-
285 bearing minerals such as feldspars. Radiometric equivalent U (eU) anomalies are commonly co-
286 located with eTh anomalies; however, because U is associated with multiple isotopes that each
287 have their own decay series, eU anomalies tend to be noisy compared to eTh and radiometric K.
288 This study is thus focused on eTh anomalies, and to a lesser degree, radiometric K anomalies.

289 Within coastal plain sediments along the eastern seaboard from Virginia to Georgia,
290 NURE aeroradiometric eTh (Figure 3) and eU generally show higher values closer to the
291 Piedmont and decreasing values with distance from the Fall Line (see also Ellefsen et al., 2015).
292 In Virginia and North Carolina, eTh anomalies are very low over Quaternary sediments.
293 However, this trend is reversed from South Carolina to northern Florida, where coast-parallel
294 bands of eTh and K highs are observed over Pleistocene and Holocene sediments. In Georgia and

295 Florida, these bands are located close to the Trail Ridge placer deposit. Farther west, in
296 Mississippi, Alabama and Tennessee, a band of eTh highs (as well as increased eU) is observed
297 along Cretaceous carbonates of the Demopolis Chalk, and in Georgia, a similar band is observed
298 over the Ocala Limestone. These latter observations are consistent with absorption of Th in
299 carbonate rocks.

300 Sinuous eTh and K highs are observed along major rivers from Virginia to Georgia,
301 corresponding to their floodplains, with K anomalies being more prominent and persisting for a
302 somewhat greater distance along those rivers than eTh anomalies. We note that K-feldspars are
303 less dense than monazite, and therefore may be carried greater distances from their sources. In
304 South Carolina and Georgia, eTh highs associated with the floodplains of the Santee, Altamaha
305 and Savannah Rivers are particularly wide. The rivers themselves, other large bodies of water,
306 and water-saturated ground, such as the Okefenokee Swamp (Ga.), Lakes Marion and Moultrie
307 (S.C.), and the Great Dismal Swamp (Va. and N.C.), show prominent eTh and K lows.

308 Anomalies within the Atlantic Coastal Plain also show regional variations, with generally
309 higher eTh in an area covering southern North Carolina, South Carolina, Georgia and eastern
310 Alabama relative to Virginia and northern North Carolina. In particular, large (> 100 km wide)
311 areas with eTh highs are present near the Fall Line from the Cape Fear arch through eastern
312 Alabama. In contrast, K anomalies are generally higher in Virginia and northern North Carolina
313 than in Coastal Plain areas farther south. The K anomalies in Alabama, Tennessee and
314 Mississippi are also elevated. Together, these data suggest a marked difference in composition
315 north and south of the Cape Fear arch. A second transition is observed near the Georgia-Alabama
316 border, where eTh highs occur mostly near the Fall Line over sands east of the state boundary
317 line and mostly in carbonate rocks to the west.

318 Over the Piedmont, eTh anomalies correspond well to geologic belts described by
319 Hatcher and Odum (1980), Secor et al. (1986), and Hibbard et al. (2002) (Figure 4). High values
320 are observed over high-grade metamorphic terranes, including the Kiokee and
321 Raleigh/Goochland belts, parts of the Pine Mountain belt and sillimanite schist areas of the Inner
322 Piedmont and Blue Ridge. Highs are also observed over certain granites such as the chains of
323 smaller granitic plutons within the Charlotte belt and Carolina slate belts. A notably broad high is
324 observed over the Petersburg Granite in Virginia. Parts of the Inner Piedmont also show local
325 highs over igneous rocks, especially in eastern Alabama and western Georgia.

326 The monazite belts described by Mertie (1953, 1979) correspond to eTh highs in
327 numerous places, but they do not correspond to a single rock type. The two western belts mostly
328 coincide with high-grade metamorphic rocks of the Inner Piedmont and Blue Ridge, as proposed
329 by Overstreet (1967). However, in central Virginia, a slight modification of the central belt so
330 that it is oriented more northerly is suggested by the radiometric data (Figure 4); we note that
331 Mertie (1979) did not have samples from this area. Additionally, the eastern belt continues from
332 metamorphic rocks of the Raleigh/Goochland belt to monazite-rich plutons of the Carolina slate
333 belt.

334 Magnetic data often show either positive or negative correlations with eTh anomalies
335 depending on rock type. Within the Charlotte belt, several plutons are associated with both eTh
336 highs and magnetic anomaly highs, particularly near the border between North and South
337 Carolina (Figure 4). In contrast, in areas with eTh highs attributable to sillimanite schist or other
338 high-grade metamorphic rock, such as the Kiokee belt or Raleigh/Goochland belt, the magnetic
339 anomalies tend to be lower. This may be associated with the destruction of magnetite in areas
340 that have undergone high-grade metamorphism (e.g., Hatcher and Zietz, 1980). We note,

341 however, that some high-grade metamorphic areas displaying eTh highs also show magnetic
342 anomaly highs (such as parts of the Inner Piedmont), perhaps due to secondary magnetite.

343 **Regional sample data**

344 Sample geochemical and geophysical data show distinct regional variations, with higher
345 concentrations of Th and La corresponding well with radiometric eTh anomalies (Figure 5; GSA
346 Data Repository). Th concentrations are greatest near the Fall Line in South Carolina amidst
347 prominent eTh highs. Intermediate Th concentrations are present in neighboring areas in North
348 Carolina and Georgia, and within a smaller area of high eTh values in eastern Alabama. Near the
349 Atlantic coast in both southeastern Georgia and northern Florida, Th concentrations are more
350 variable, with some samples showing medium concentrations and others showing lower
351 concentrations. In Virginia, where aeroradiometric eTh is relatively low, La and Th also show
352 decreased concentrations in heavy mineral separates. These variations are also reflected in field
353 site data (Table 1). Together, these data provide further evidence that the composition of the
354 heavy mineral assemblage contributes significantly to the magnitude of eTh anomalies.

355 The magnetic susceptibility map also shows regional variations, but with more local
356 variability. Near the Fall Line, higher susceptibility values are observed in eastern Alabama and
357 in some locations north of the Cape Fear arch (Figure 5). In areas closer to the coast, these values
358 are more mixed. Correspondences with minerals are more difficult to ascertain because trace
359 amounts of highly magnetic minerals, such as magnetite, can strongly impact magnetic
360 susceptibility. However, for most samples, magnetic susceptibility is correlated with Fe content
361 (see GSA data repository). Regional magnetic anomalies do not show correspondences with
362 magnetic susceptibility values of heavy mineral separates, probably because they are dominated

363 by sources in the crystalline basement. These regional variations in magnetic susceptibility are
364 examined in more detail using ground surveys, discussed below.

365 Rutile concentrations, which were estimated using X-ray diffraction, show broad, distinct
366 regional variation, with highest concentrations near the Fall Line from south of the Cape Fear
367 arch through Georgia (Figure 5). The rutile concentrations show little to no correlation with Ti
368 concentrations, which are high over most of the southeastern U.S., probably because Ti appears
369 in other minerals such as ilmenite. The rutile concentrations show a nearly inverse correlation
370 with magnetic susceptibility (with exception of Tennessee, which is low in both). We note that
371 rutile is sourced predominantly from high-grade metamorphic rocks (Force, 1980), and that high-
372 grade metamorphism typically has a destructive effect on magnetite. We also note that many
373 areas with increased rutile show increased Th and monazite, suggesting that monazite in those
374 areas may also have been formed under higher grade metamorphic conditions. Staurolite, which
375 is primarily found in low- to mid-grade metamorphic rocks, is more variable. Areas near the Fall
376 Line in South Carolina are notably low in staurolite while areas in Virginia and northern North
377 Carolina generally have greater staurolite content.

378 The distributions of Th and monazite concentrations, rutile concentrations and magnetic
379 susceptibility suggest that the study area can be divided into sub-regions with the following
380 properties (see also Table 2):

- 381 1. Virginia and northern North Carolina (except near major rivers): characterized by low
382 monazite and Th concentrations except near major rivers, higher magnetic susceptibility
383 and mostly low rutile content.
- 384 2. Southern North Carolina (near the Cape Fear arch): characterized by mixed magnetic
385 susceptibility and concentrations of monazite and rutile.

- 386 3. Near the Fall Line from South Carolina through Georgia: characterized by high Th and
387 monazite, low magnetic susceptibility and mostly high rutile.
- 388 4. Eastern Alabama near the Fall Line: characterized by high Th and monazite, high
389 magnetic susceptibilities and low rutile.
- 390 5. Coastal South Carolina, Georgia, and northern Florida: characterized by highly variable
391 from sample to sample.
- 392 6. Western Tennessee: characterized by low Th, low magnetic susceptibility, and low rutile.

393 **Detailed surveys**

394 High-resolution surveys provide a key component of interpretation of widely spaced
395 airborne gamma spectrometry data by providing detailed views of local variation that cannot
396 otherwise be resolved. This includes the airborne total count data collected over South Carolina
397 and ground surveys at various locales.

398 *Airborne total count data over South Carolina*

399 The high-resolution airborne total count data over South Carolina (Figure 6) provide a
400 detailed picture of radiometric anomalies. These anomalies correspond well with the NURE eTh
401 maps, suggesting that in South Carolina the total count signature is dominated by Th and perhaps
402 U, because the two are commonly associated in certain minerals.

403 Within the Piedmont, the total count data show distinct circular highs over various
404 plutons. Broad total count highs are also observed in the presence of sillimanite schist, reflecting
405 high-grade metamorphism that produced monazite. This includes a wedge-shaped high that
406 exists where the Kiokee belt crops out near the Fall Line. Near the Santee/Broad/Congaree River
407 system, 1-2 km wide striations parallel to the river system are observed, especially near the
408 Winnsboro pluton and the Santuck granite, suggesting the transport and deposition of Th-rich

409 sediments within the associated riverbed. Such striations are not observed, however, near smaller
410 rivers, even near the Th-rich sillimanite schist of the Inner Piedmont.

411 Coastal Plain sediments adjacent to the Kiokee belt show particularly high total count
412 values for a distance of about 75 km downslope, toward the southeast. They also extend for
413 about 75 km eastward from the edge of the Kiokee belt outcrop, reaching past the Santee River
414 and downslope of areas near the Fall Line. At distances more than 75-100 km from the Fall Line,
415 total count values are low (Figure 6) until Quaternary sediments are reached (see Figure 1).
416 Highs are also observed along the floodplains of the Santee and PeeDee Rivers. Between these
417 rivers, in the Cretaceous Peedee Formation, numerous 25-50-km long striations oriented
418 similarly to the northwest-southeast floodplains are observable. While total count lows likely
419 correspond to smaller fluvial systems, other highs may reflect differences in sand composition.
420 These striations are not present in the Piedmont. Near the coast, the total count map exhibits
421 anomalies alongside northeast-southwest coast-parallel Pleistocene ridges.

422 ***Modern Beaches from Florida to North Carolina***

423 Several modern beaches in different parts of the southeastern U.S. were surveyed (Figure
424 1). The beaches provide easy access to samples and, in most cases, visual confirmation of heavy
425 mineral sand presence. At both Folly Beach, South Carolina, and Little Talbot Island, Florida,
426 data grids were obtained by surveying troughs in rows of linear sand dunes at Little Talbot Island
427 and by utilizing a wide beach area at Folly Beach (Figure 7). At two other sites, the Outer Banks,
428 North Carolina, and Cumberland Island, Georgia, single profiles along the shore were obtained
429 (Figure 8).

430 The highest eTh values were observed at Folly Beach and Little Talbot Island. Significant
431 (up to ~5 nT) magnetic anomalies in locations near eTh anomalies were observed at Folly Beach

432 (Figure 7), whereas smaller 1-2 nT anomalies were observed at Little Talbot Island. This is
433 consistent with slightly increased magnetic susceptibilities of heavy mineral separates for Folly
434 versus Little Talbot Island. At Cumberland Island, both eTh and XRF measurements of Th were
435 generally lower (Figure 8). A clear magnetic anomaly is not apparent, but there is suggestion of
436 slightly greater variation of magnetic anomalies in areas where eTh is higher (the variations may
437 represent noise, however). Magnetic susceptibility and Th content of heavy mineral separates are
438 similar for both Cumberland and Little Talbot Islands, so we infer that heavy mineral
439 concentrations are lower in the Cumberland Island survey area than the Little Talbot Island
440 survey area.

441 XRF analyses of surface-grab samples from these three sites show strong correlations
442 between Th content and eTh anomalies. Ti, Fe and Zr concentrations correlate well with both Th
443 concentrations and eTh, indicating that the eTh anomalies not only represent Th content, but that
444 they also reflect enriched concentrations of heavy minerals. There are some exceptions, mostly at
445 Cumberland Island, presumably due to layering of heavy minerals that can cause differences
446 between surface sands and those just a few inches below.

447 The Outer Banks survey data showed notably different characteristics from those of the
448 more southern beaches. The eTh measurements generally fell within sensitivity and precision
449 levels of the instrument and sample XRF Th concentrations were all below 35 ppm. However,
450 magnetic anomalies show much more variation (10-15 nT). The wavelength of these anomalies
451 is too short to represent rocks in the crystalline basement, which are several kilometers deep.
452 These results are consistent with heavy mineral concentrate measurements that show higher
453 magnetic susceptibilities (5.5×10^{-3} SI) than those from beaches farther south, but also much
454 lower Th content. Although the magnetic anomalies don't directly correspond with grab-sample

455 measurements of Th, Ti or Fe, there is generally greater short-wavelength (10-50 m length scale)
456 variation in areas where Th concentrations are higher, indicating shallower magnetic sources and
457 further suggesting that the anomalies represent heavy mineral sand layers.

458 *Aurelian Springs, North Carolina*

459 The Aurelian Springs deposit is located within Tertiary terrace deposits of northern North
460 Carolina, close to the Fall Line (Figure 9). This area has been evaluated for a future mineral
461 sands mining operation that would produce ilmenite and zircon by Iluka Resources, Inc. We
462 conducted a single-line profile magnetic and radiometric survey along a dirt path where drill
463 samples had been obtained by Iluka Resources, Inc., with a spacing of roughly 60 m (Figure 9).
464 The drill data show highest heavy mineral concentrations toward the western part of the profile.
465 Total count anomalies were collected in “continuous” mode using the RS-125, and were very
466 similar to eTh measurements from 1-minute assays. Radiometric eTh values are not very high,
467 but they do show elevated values where heavy mineral concentrations are higher.

468 Magnetic data also showed higher values where heavy mineral concentrations are
469 present, but the magnetic highs are somewhat offset from the eTh highs. This may partly be due
470 to the fact that magnetic data can image deeper sources than radiometric data. There may also be
471 a contribution from basement rock, which is less than 200 m deep in this area. The latter
472 possibility is supported by the magnitude of the highs, exceeding 200 nT, which is very high for
473 sedimentary sources.

474 We also obtained two depth profiles of samples along the survey, one within the deposit,
475 and one farther east outside of the deposit. Magnetic susceptibility and geochemistry of bulk
476 sands as a function of depth were estimated using a SM-30 field susceptibility meter and ICP-
477 AES-MS, respectively. At the site within the deposit, heavy mineral concentrations range from 3

478 to 4%. Ti was elevated near the surface (Figure 10), corresponding to increased heavy mineral
479 concentrations there. Th was also slightly elevated mainly in the upper 1 m, with a maximum
480 value near 35 ppm near a depth of 50 cm. Magnetic susceptibility values were notably high in the
481 upper 30 cm of the hole but decreased abruptly with depth; they did not show a correspondence
482 with heavy mineral content. This may be an effect of leaching or alteration of magnetite through
483 the soil column. Nonetheless, magnetic susceptibility laboratory measurements of heavy mineral
484 separates from Aurelian Springs were $\sim 14.34 \times 10^{-3}$ SI, which is comparable to igneous rocks. It
485 is thus difficult to determine which part of the magnetic signal might be due to heavy minerals
486 and which part is due to basement rock. Outside of the deposit area, eTh and magnetic anomalies
487 were lower, along with heavy mineral concentrations, Ti, Th, and magnetic susceptibility. To
488 further explore the utility of these methods, an additional grid survey was conducted over a wide
489 area on a nearby farm. Results were similar (GSA Online Repository).

490 *Other sites in South Carolina*

491 Cheraw State Park is located within the band of eTh highs along the Fall Line in South
492 Carolina and is underlain by the Cretaceous Peedee Formation. Ground radiometric surveys
493 exhibit intermediate eTh values in that area (Table 2, GSA Online Repository). Two hand-auger
494 holes of ~80 cm depth were obtained, one within the eTh highs (CH A1) and one within an eTh
495 low (CH A2). Heavy mineral concentrations within these sites were low (<1 %), however, bulk
496 sands within CH A1 showed significant Th (Figure 10) and La concentrations (up to 150 ppm).
497 These are higher than those observed at Aurelian Springs (up to 35 and 50 ppm for Th and La,
498 respectively) even though heavy mineral concentrations there were 3-4%.

499 The Francis Marion National Forest survey site (Figure 1) is located within radiometric
500 highs associated with the Santee River and is part of the Pleistocene Socaste Formation. Ground

501 radiometric eTh surveys show intermediate values there as well, but not as high as those at
502 Cheraw (Table 2). A hand-auger hole obtained within local radiometric eTh highs also showed
503 very small amounts (< 1%) of heavy mineral sands, but bulk sand Th and La values were 20-23
504 ppm and 60-67 ppm, respectively, on par with Aurelian Springs (Figure 10) in spite of much
505 lower heavy mineral concentrations.

506 Magnetic anomalies show little relation to eTh anomalies at these sites and magnetic
507 susceptibilities of auger samples were very low ($<0.05 \times 10^{-3}$ SI). Within Cheraw, magnetic
508 anomalies over the area vary up to 400-500 nT, whereas within Francis Marion they vary 15-20
509 nT over the respective survey areas. The magnetic anomalies at both sites likely reflect basement
510 rock, noting that the crystalline basement is shallower at Cheraw, reducing the distance to the
511 magnetic source.

512 *North of Folkston, Georgia*

513 The Trail Ridge and Folkston deposits are located along a >200-km long Pleistocene
514 ridge extending from northern Florida to southern Georgia, oriented parallel to the Atlantic
515 Coast. This ridge was likely once a barrier island (Force and Rich, 1989). Parts of these deposits
516 are actively being mined for ilmenite, rutile and zircon. We conducted ground radiometric and
517 magnetic surveys over an area north of Folkston, corresponding with Southern Ionics drill holes
518 spaced ~100-200 m along several profiles (Figure 11). Continuous measurements using the
519 Gamma Surveyor showed a direct correspondence between eTh and estimated heavy mineral
520 concentrations, although eTh values were low compared to other field sites. Total count data
521 showed similar patterns. The magnetic data, on the other hand, exhibited a rather different
522 pattern. Magnetic anomalies were lowest in areas where the deposit is thickest (determined by
523 models based on drill hole data). The base of the heavy mineral sands is marked by hard,

524 consolidated Fe-rich sedimentary rock referred to as “hardpan.” Measured magnetic
525 susceptibilities of samples of this rock were very high ($>20 \times 10^{-3}$ SI), suggesting that the
526 magnetic anomalies reflect the shape of the hardpan surface. The magnetic susceptibility of the
527 heavy mineral separates was lower, $\sim 0.98 \times 10^{-3}$ SI.

528 ***James River, Virginia***

529 Along the James River east of the Fall Line, small crescent-shaped beaches commonly
530 contain visible heavy mineral concentrations (see Berquist et al., 2015). These areas were too
531 small for geophysical surveys, but spot radiometric assays at two sites showed the highest eTh
532 readings of all surveys. Concentrations of heavy minerals were very high at both sites, and the
533 second site was almost 100% heavy minerals; a grab sample of bulk sands had a density of 2.9
534 g/cm^3 . The high eTh readings are then likely due to the enriched concentration of heavy
535 minerals. Magnetic susceptibilities were also remarkably high at these sites. Samples showed
536 low to negligible amounts of rutile and staurolite.

537 ***Relations to local geologic features***

538 Geophysical data provide much denser coverage of an area than is possible with sampling
539 or drilling. They thus have the potential to highlight relations to geologic features and can
540 provide insights into processes that lead to heavy mineral concentrations. The ground
541 radiometric surveys show anomalies that correspond to several geologic features. For example, at
542 Little Talbot Island, the highest eTh values were observed along a stretch of beach that is
543 bounded by an eroding cliff wall and thus only accessible during low tides (Figure 7). The sand
544 dunes at Little Talbot Island had much lower eTh values, except at their northern end where they
545 approach the modern shore. In contrast, on Cumberland Island, higher eTh values were observed
546 mainly in overwash areas and in a bend of the shoreline where the beach was very narrow. At

547 Cheraw State Park, eTh values were high along topographic gradients that likely represent
548 ancient riverbeds, and peaked near the apparent confluence of two riverbeds (GSA Online
549 Repository). While an in-depth analysis of sedimentary processes in these three areas is beyond
550 the scope of this work, together the geophysical data suggest the importance of erosional
551 processes at Little Talbot Island (e.g., through entrainment sorting and the formation of lag
552 deposits), fluvial transport and deposition at Cheraw State Park, and both at Cumberland Island.

553 **DISCUSSION**

554 **Regional distribution of Th and REE-bearing minerals**

555 Regional variations in Th, monazite and associated xenotime are evident in radiometric,
556 geochemical, and mineralogical datasets. Within southeastern U.S. Coastal Plain sediments,
557 NURE eTh anomalies are generally higher in areas near the Fall Line from southern North
558 Carolina through eastern Alabama and in Quaternary sediments near the Atlantic Coast from
559 South Carolina through northern Florida. Such anomalies are also observed along most major
560 alluvial plains, but they generally cover wider areas in South Carolina and Georgia.

561 Sections of the Coastal Plain with high eTh values that lie near the Fall Line (Figure 12)
562 form an area greater than 33,000 km². Pleistocene ridges and fluvial flood plains, as well as
563 modern beaches from South Carolina to Georgia also exhibit high eTh and add an additional
564 2,600 km². The possible total resource of monazite and xenotime in these areas is significant. For
565 example, an area south of Folkston near Boulonge, Fla., covering ~4 km² (~1,000 acres) was
566 mined from 1974-1978 to about 5 m depth. This area contained about 4% heavy minerals of
567 which monazite composed 0.3-0.4% (Staatz et al., 1980), suggesting ~40,000 metric tons of
568 monazite for the area. Coastal sand-silt deposits of northeastern Florida were estimated to
569 contain 330,000 metric tons of monazite, of which 198,000 metric tons represent REE oxides

570 (Staatz et al., 1980). Together, these represent a very small percentage of the region covered with
571 radiometric eTh highs that likely correspond to heavy mineral sand deposits.

572 **Regional variations in source rock type**

573 Regional variations in monazite and xenotime are correlated with regional variations in
574 co-minerals and magnetic susceptibility (Tables 1-2, Figure 5), which in turn are associated with
575 different source rock types. This suggests that it is possible to gain information regarding the
576 sources of the heavy mineral sands. Monazite is usually observed in both high-grade
577 metamorphic rocks and many types of igneous rocks, rutile is primarily observed in high-grade
578 metamorphic rocks and staurolite is usually observed in low- to mid-grade metamorphic rocks
579 (e.g., Force, 1980; Force, 1981).

580 Elevated magnetic susceptibilities are observed in igneous, low-grade metamorphic, and
581 high-grade metamorphic rocks. However, in igneous and low-grade metamorphic rocks they are
582 typically associated with magnetite, hematite and maghemite while in high-grade metamorphic
583 rocks hematite and/or maghemite are rarer, and elevated susceptibilities are usually attributable
584 to magnetite (Grant, 1984). Once magnetite is eroded into sediments, it is typically altered over
585 time through oxidation and/or other weathering processes. Elevated magnetic susceptibilities in
586 older sediments are thus commonly attributable to hematite, maghemite, and to a lesser degree,
587 ilmenite. Sediments with higher magnetic susceptibilities are thus usually associated with
588 igneous and/or lower-grade metamorphic source rocks, unless they were recently eroded.

589 Regional variations in the heavy mineral assemblage suggest the following distribution of
590 dominant source rocks (summarized in Table 1 and Figure 12):

- 591 - Heavy mineral sands in Virginia and northern North Carolina away from major river
592 systems appear to be derived mainly from low- to medium- grade metamorphic rocks

593 based on lower rutile, increased staurolite, lower monazite and high magnetic
594 susceptibilities. This appears to be the case for sediments both near to and distal from the
595 Fall Line.

- 596 - In southern North Carolina near the Fall Line, a combination of intermediate rutile,
597 variable staurolite, mostly high magnetic susceptibility, and mostly high monazite
598 concentrations suggests a combination of high-grade metamorphic rocks and igneous
599 rocks as a source of monazite.
- 600 - In South Carolina and eastern Georgia near the Fall Line, high rutile, lower staurolite,
601 high monazite, and low magnetic susceptibilities suggest that the heavy minerals are
602 derived from high-grade metamorphic rocks.
- 603 - In western Georgia and eastern Alabama near the Fall Line, decreased rutile, mixed
604 staurolite, and high magnetic susceptibilities combined with high monazite
605 concentrations suggest a primarily igneous source for monazite, but perhaps with mixing
606 from nearby areas.
- 607 - In eastern Tennessee and Mississippi, lower concentrations of denser minerals suggest
608 that these heavy mineral sands were transported a long distance; variable rutile, magnetic
609 susceptibility, and other properties also suggest significant mixing and/or differentiation
610 during transport.
- 611 - In areas within ~100 km from the coast between northern Florida and South Carolina, the
612 local variability of geophysical and geochemical properties of samples from these areas is
613 high, suggesting mixing from multiple sources and differentiation of minerals during
614 transport.

615 - Coastal plain sediments sampled from near the James River, Virginia, are low in rutile
616 and staurolite, highly magnetic, and high in monazite, as inferred from Th content. This
617 combination is consistent with an igneous source such as the Petersburg Granite, which
618 the James River traverses farther inland. These sediments also showed fewer signs of
619 alteration, suggesting they were more recently eroded.

620 **Implications for sedimentary provenance and deposit formation**

621 The regional variation in inferred source rock type allows us to consider the likely
622 provenance of the heavy mineral sands. This is most feasible at the scale of the Piedmont and
623 Blue Ridge belts since they are defined by different degrees of metamorphism and variable
624 presence of igneous rocks. We find that the Atlantic Coastal Plain sub-regions near the Fall Line
625 correspond best to proximal Piedmont/Blue Ridge belts that border those sediments (Figure 12).

626 For example:

- 627 - In Virginia and northern North Carolina, Atlantic Coastal Plain sediments border the
628 Piedmont's 10-20-km wide Eastern slate belt; properties of both are consistent with low
629 grade metamorphism. These sediments show little resemblance to the 20-60-km wide
630 high-grade metamorphic Raleigh/Goochland belt farther inland.
- 631 - In South Carolina and Eastern Georgia near the Fall Line, heavy mineral sand properties
632 suggest high-grade metamorphism; these sediments border the 5-20-km wide high-grade
633 metamorphic Kiokee and Uchee belts. Areas farther inland comprise mostly low-grade
634 metamorphic and igneous rocks.
- 635 - In southern North Carolina near the Fall Line, the coastal plain sediments border the
636 Lilesville pluton, which is associated with an eTh high (Figure 6) and thus likely to have
637 higher concentrations of monazite and xenotime. Mixing of sediments derived from both

638 igneous and high-grade metamorphic rocks is suggested for this area. Heavy mineral
639 sands from areas near the Kiokee belt may contribute to this area via northeasterly
640 transport.

641 - In eastern Alabama near the Fall Line, coastal sediments border a complex series of
642 Piedmont/Blue Ridge units that include granodiorite and monzonite, granite, gneisses,
643 amphibolite, and schist, consistent with both igneous and mixed sources. Most areas
644 farther inland are characterized by high-grade metamorphism although there are also
645 intrusions present.

646 The belts further inland appear to contribute little to heavy mineral assemblages near the
647 Fall Line, even though they crop out over a much wider area than those near the Fall Line. The
648 dominant source of heavy mineral sands near the Fall Line thus appears to be those units that
649 formed the ancient rocky coast during opening of the Atlantic Ocean. This in turn suggests that
650 coastal processes contributed much more to heavy mineral sand deposit formation than alluvial
651 processes since the latter would have delivered more sediment eroded from rocks farther inland.
652 This scenario is similar to heavy mineral sand deposits in the Eucla and Murray Basins in
653 Australia and along the coast of Brazil near the Atlantides belt, where strong correlations
654 between beach placer composition and hinterland rocks have been observed (Keeling et al.,
655 2015; Leonardos, 1974; Reid et al., 2013). In contrast however, there are Quaternary beach
656 deposits within the Perth Basin and on the east coast of Australia where an extensive history of
657 sediment reworking, longshore transport, and possibly tectonic uplift results in distinct
658 differences between placer deposits and neighboring crystalline rock (Roy, 1999; Sircombe and
659 Freeman, 1999).

660 While coastal processes appear to have dominated hard rock erosion and formation of
661 heavy mineral sand deposits, the influence of alluvial processes can be observed at a more local
662 scale within ancient and modern riverbeds. The narrow width of radiometric K and eTh highs
663 along major river beds (Figure 3) strongly suggest that the influence of alluvial processes is
664 spatially limited, as might be expected within river valleys. This has been observed in studies of
665 modern coastal sediments in the mid-Atlantic (Prusak and Mazzullo, 1987) and in part of the Old
666 Hickory deposit in southern Virginia (Newton and Romeo, 2006). We note that intermediate eTh
667 anomalies associated with major rivers in Virginia and North Carolina may be due to small
668 amounts of monazite and xenotime derived from the Raleigh/Goochland belt (inland of the
669 Eastern slate belt). Higher and wider eTh anomalies are associated with rivers further south, such
670 as the Santee River in South Carolina. The latter traverses both the Kiokee belt and monazite-
671 rich intrusions of the Charlotte belt and may contribute to sediment deposition at Folly Beach.
672 Additional contribution might be derived from the high-Th rocks of the southern Inner Piedmont.

673 Heavy mineral concentrates in areas distal from the Piedmont, including coastal areas,
674 Mississippi, and Tennessee suggest mixed sources. This is likely due to repeated reworking of
675 sands and coast-parallel transport by longshore currents over time. We note, however, that
676 Quaternary sediments in South Carolina, Georgia and Florida are generally richer in monazite
677 and xenotime than their counterparts in northern North Carolina and Virginia. More generally,
678 radiometric eTh anomalies are generally higher over Cenozoic sands south of the Cape Fear
679 arch, and Bern et al. (2016) noted gradual decreases in monazite and xenotime of bulk sands with
680 distance from the Fall Line. Together, these data suggest in areas south of the Cape Fear arch,
681 elevated monazite and xenotime are maintained with distance from the Fall Line, albeit as
682 smaller percentages of bulk sands. We hypothesize that repeated reworking, transport, and

683 deposition of sands as the shoreline gradually moved from the ancient rocky coast resulted in an
684 “inheritance” of composition. This inheritance becomes diluted, however, with mixing by
685 longshore currents. Remarkably, if such inheritance is indeed present, it suggests that a very
686 small portion of the Piedmont and Blue Ridge provinces, i.e., that which formed the rocky coast
687 during Mesozoic opening, may be the dominant source of heavy minerals in the Atlantic Coastal
688 Plain. Future work such as dating of detrital zircons and monazite may provide further insight
689 into this possibility.

690 **Implications for geophysical survey sensitivity**

691 Geophysical methods can be used as exploration tools, but broad, regional differences in
692 heavy mineral composition suggest how these tools might be “calibrated” when surveying in
693 different areas for heavy mineral concentrates. For example, radiometric eTh anomalies in areas
694 south of the Cape Fear arch such as those at Cheraw, S.C. typically reflect a heavy mineral
695 composition with elevated monazite and xenotime, but the overall heavy mineral percentage is
696 likely to be small compared to the same anomaly farther north in Aurelian Springs, N.C. In
697 contrast, magnetic ground surveys south of the Cape Fear arch are generally lower in magnitude,
698 and a magnetic anomaly observed in say Folly Beach, S.C. will be associated with a much higher
699 heavy mineral sand percentage than the same anomaly in the Outer Banks, N.C. However,
700 magnetic survey data can be complicated by weathering, alteration and leaching of magnetic
701 minerals. Furthermore, care must be taken to distinguish sources from within the sediments and
702 sources within the underlying crystalline basement. In general, beach or offshore environments
703 may provide greater consistency when using magnetic data to image heavy mineral
704 concentrations.

705 **CONCLUSIONS**

- 706 1. Combined geochemical, mineralogical and ground geophysical survey data support an
707 interpretation of broad eTh highs in NURE aeroradiometric data indicating the occurrence
708 of monazite- and xenotime-bearing heavy mineral sands across the coastal plain of the
709 southeastern United States.
- 710 2. Regional radiometric data support previous studies at local scales which show that
711 geophysical surveys can help identify and delineate heavy mineral concentrations.
- 712 3. The sensitivity of each geophysical method varies according to broad regional differences
713 in the heavy mineral assemblage, with magnetic methods showing greater response to
714 heavy minerals north of the Cape Fear arch in North Carolina and radiometric methods
715 showing greater response farther south.
- 716 4. Characterization of heavy mineral assemblages is aided by analyses of geophysical,
717 geochemical, and mineralogical properties of heavy mineral separates. These variations
718 show a strong correlation between the composition of coastal plain heavy mineral sands
719 near the Fall Line and neighboring crystalline rock types, similar to placer deposits
720 observed in several Australian basins and along Brazil's coastline near metamorphic rocks.
721 In contrast, coastal areas of the southeastern U.S. farther from the Fall Line show heavy
722 mineral concentrations that are more mixed and more fractionated, resembling coastal
723 Quaternary placer deposits in Australia.
- 724 5. The correlation between heavy mineral sands and units of the ancient rocky coast suggests
725 that coastal processes dominate heavy mineral sand deposition and accumulation in those
726 areas. This is supported by relatively narrow radiometric anomalies associated with major
727 rivers, indicating limited spatial influence of alluvial processes.

728 6. A dominance of coastal processes in turn suggests that smaller areas of the Piedmont and
729 Blue Ridge provinces contribute more to heavy mineral sands in the adjacent coastal plain
730 than previously assumed. With increasing distance from the Piedmont, compositions
731 become more mixed, especially within 100 km of the Atlantic coastline. However, a small
732 degree of compositional “inheritance” appears to be maintained.

733 **ACKNOWLEDGEMENTS**

734 We thank C. Ailes, B. Burton and J. Reitman for their help with collecting the ground
735 geophysical survey data. H. Lowers assisted with sample preparation and analysis. We thank
736 Iluka resources, Inc., and Southern Ionics, Inc., for providing access to private lands and for
737 sharing drill data in areas surveyed. We thank the Florida Department of Agriculture, the Florida
738 Park Service, the Georgia Department of Natural Resources, the National Park Service, South
739 Carolina State Parks, and the U.S. Forest Service for providing access to various survey areas.
740 We especially appreciate logistical assistance received from the National Park Service at
741 Cumberland Island and the Florida Park Service at Little Talbot Island. Thoughtful discussions
742 with Andrew Grosz, J. Wright Horton, Jr., and C. Saunders contributed to this manuscript. We
743 thank Jeff Mauk, Mike Thomas and an anonymous reviewer for detailed and thoughtful reviews
744 that helped the manuscript. This effort was supported by the U.S. Geological Survey Mineral
745 Resources Program. Any use of trade, firm, or product names is for descriptive purposes only
746 and does not imply endorsement by the U.S. Government.

747 **REFERENCES**

- 748 Bern, C.R., Shah, A.K., Benzel, W.M., and Lowers, H.A., 2016, The distribution and
749 composition of REE-bearing minerals in placers of the Atlantic and Gulf coastal plains,
750 USA: *Journal of Geochemical Exploration*, v. 162, p. 50-61.
- 751 Berquist, C.R., Shah, A.K., and Karst, A., 2015, Placer deposits of the Atlantic Coastal Plain:
752 Stratigraphy, sedimentology, mineral resources, mining and reclamation: Guidebook
753 Series of the Society of Economic Geologists, Inc., Guidebook 50, 48 p., ISSN 2374-
754 6955 online.
- 755 Darby, D.A., 1984, Trace elements in ilmenite: A way to discriminate provenance or age in
756 coastal sands: *Geological Society of America Bulletin*, v. 95, p. 1208-1218.
- 757 Dryden, L., 1958, Monazite in part of the southern Atlantic Coastal Plain: U.S. Geological
758 Survey Bulletin 1042-L, p. 393-429.
- 759 Duval, J.S., Carson, J.M., Holman, P.B., and Darnley, A.G., 2005, Terrestrial radioactivity and
760 gamma-ray exposure in the United States and Canada: U.S. Geological Survey Open-File
761 Report 2005-1413. Available online only at <http://pubs.usgs.gov/of/2005/1413/>.
- 762 Ellefsen, K., Van Gosen, B.S., Fey, D., Budahn, J. Smith, S., and Shah, A.K., 2015, First steps of
763 integrated spatial modeling of titanium, zirconium, and rare earth element resources
764 within the Coastal Plain sediments of the southeastern United States: U.S. Geological
765 Survey Open-file report 2015-1111, 40 p.
- 766 Force, E.R., 1980. The provenance of rutile: *Journal of Sedimentary Petrology*, v. 50, p. 485-488.
- 767 Force, E.R., 1991, Geology of titanium-mineral deposits: *Geological Society of America Special*
768 Paper 259, 112 p.

769 Force, E.R., and Rich, F.J., 1989, Geologic evolution of Trail Ridge eolian heavy-mineral sand
770 and underlying peat, northern Florida: U.S. Geological Survey Professional Paper 1499,
771 16 p.

772 Force, E.R., Grosz, A.E., Loferski, P.J., and Maybin, A.H., 1982, Aeroradioactivity maps in
773 heavy-mineral exploration—Charleston, South Carolina, area: U.S. Geological Survey
774 Professional Paper 1218, 19 p., 2 plates.

775 Garnett, R. H. T., and Bassett, N. C., 2005, Placer deposits, in Hedenquist, J. W., Thompson, J.
776 F. H., Goldfarb, R. J., and Richards, J. P., eds., Economic Geology one hundredth
777 anniversary volume 1905-2005: Littleton, Colorado, Society of Economic Geologists, p.
778 813-843.

779 Grant, F.S., 1984, Aeromagnetism, geology and ore environments, 1. Magnetite in igneous,
780 sedimentary and metamorphic rocks: An overview: *Geoexploration*, v. 23, p. 303-333.

781 Grosz, A.E., 1983, Application of total-count aeroradiometric maps to the exploration for heavy-
782 mineral deposits in the Coastal Plain of Virginia: U.S. Geological Survey Professional
783 Paper 1263, 20 p., 5 plates.

784 Grosz, A.E., 1993, Use of geochemical surveys in Ti-Hf-REE-Th-U placer exploration—A mid-
785 Atlantic-States example (Chapter R), in Scott, R.W., Jr., Detra, P.S., and Berger, B.R.,
786 eds., *Advances related to United States and international mineral resources—Developing*
787 *frameworks and exploration technologies*: U.S. Geological Survey Bulletin 2039, p. 181–
788 188.

789 Grosz, A.E., Cathcart, J.B., Macke, D.L., Knapp, M.S., Schmidt, Walter, and Scott, T.M., 1989,
790 Geologic interpretation of the gamma-ray aeroradiometric maps of central and northern
791 Florida: U.S. Geological Survey Professional Paper 1461, 48 p., 5 plates.

792 Grosz, A.E., Francisco, C.S.J., Jr., and Reid, J.C., 1992, Heavy-mineral concentrations
793 associated with some gamma-ray aeroradiometric anomalies over cretaceous sediments in
794 North Carolina: implications for locating placer mineral deposits near the fall zone:
795 USGS Open-File Report 92-396, 27 p.

796 Grosz, A.E., and Schruben, P.G., 1994, NURE Geochemical and Geophysical Surveys –
797 Defining prospective terranes for United States Placer Exploration: U.S. Geological
798 Survey Bulletin 2097, 9 p., 2 plates.

799 Hatch, G.P., 2012, Dynamics in the global market for rare earths: *Elements*, v. 8, no. 5, p. 341–
800 346.

801 Hatcher, R.D. and Odum, A.L., 1980, Timing of thrusting in the southern Appalachians, USA:
802 model for orogeny?: *Journal of the Geological Society of London*, v. 137, p. 321-327.

803 Hatcher, R.D. and Zietz, I. 1980, Tectonic implications of regional aeromagnetic and gravity
804 data from the southern Appalachians: *in* Wones, D.R., ed., *The Caledonides in the USA.:*
805 *IGCP Project 27: Caledonide Orogen: Virginia Tech Department of Geological Sciences,*
806 *Memoir*, v. 2, p. 235-244.

807 Hibbard, J.P., Stoddard, E.F., Secor, D.T., and Dennis, A.J., 2002, The Carolina Zone: overview
808 of Neoproterozoic to Early Paleozoic peri-Gondwanan terranes along the eastern Flank of
809 the southern Appalachians: *Earth-Science Reviews*, v. 57, p. 299-339.

810 Hoatson, D.M., Jaireth, S., and Mieзитis, Y., 2011, The major rare-earth-element deposits of
811 Australia— Geological setting, exploration, and resources: *Geoscience Australia*, 204 p.

812 Horton, J.W. and Dicken, C.L., 2001, Preliminary Geologic Map of the Appalachian Piedmont
813 and Blue Ridge, South Carolina Segment: U.S. Geological Survey, Open-File Report 01-
814 298, CD-ROM.

815 Keeling, J.L., Reid, A.J., Hou, B., Pobjoy, R., 2015. Provenance of zircon in heavy mineral sand
816 deposits, western Murray Basin: Department of State Development, South Australia,
817 Report Book, 2015/00031, 62 p.

818 Leonardos Jr., O.H., 1974, Origin and provenance of fossil and recent monazite deposits in
819 Brazil: *Economic Geology*, v. 69, p. 1126-1128.

820 Long, K.R., Van Gosen, B.S., Foley, N.K., and Cordier, D., 2010, The principal rare earth
821 elements deposits of the United States—A summary of domestic deposits and a global
822 perspective: U.S. Geological Survey Scientific Investigations Report 2010–5220, 96 p.,
823 <http://pubs.usgs.gov/sir/2010/5220/>.

824 Meleik, M.L., Fouad, K.M., Wassef, S.N., Ammar, A.A. and Dabbour, G.A., 1978, Aerial and
825 ground radiometry in relation to the sedimentation of radioactive minerals in the
826 Damietta beach sands, Egypt: *Economic Geology*, v. 73, p. 1738-1748.

827 Mertie, Jr., J.B., 1953, Monazite deposits of the Southeastern Atlantic States: U.S. Geological
828 Survey Circular 237, 31 p.

829 Mertie, Jr., J.B., 1979, Monazite in the granitic rocks of the southeastern Atlantic states – an
830 example of the use of heavy minerals in geologic exploration: U.S. Geological Survey
831 Professional Paper 1094, 86 p., 1 plate.

832 Mohanty, H., 2015, Country's only monazite processing plant goes on stream: *Business*
833 *Standard*, October 9, 2015, available online at [http://www.business-](http://www.business-standard.com/article/companies/countrys-only-monazite-processing-plant-goes-on-stream-115100900778_1.html)
834 [standard.com/article/companies/countrys-only-monazite-processing-plant-goes-on-](http://www.business-standard.com/article/companies/countrys-only-monazite-processing-plant-goes-on-stream-115100900778_1.html)
835 [stream-115100900778_1.html](http://www.business-standard.com/article/companies/countrys-only-monazite-processing-plant-goes-on-stream-115100900778_1.html), accessed Dec. 21, 2015.

836 Mudge, S., and Teakle, M., 2003, Geophysical exploration for heavy-mineral sands near
837 Mindarie, South Australia: Australian Society of Exploration Geophysicists (ASEG)
838 Extended Abstracts 2003, no. 3, p. 249–255.

839 Naeser, N.D, Naeser, C.W., Newell, W.L., Southworth, S., Weems, R., and Edwards, L., 2006,
840 Provenance studies in the Atlantic coastal plain: What fission-track ages of detrital
841 zircons can tell us about the erosion history of the Appalachians: Geological Society of
842 America Abstracts with Programs, Vol. 38, No. 7, p. 503.

843 Neathery, T. L., Bentley, R. D., Higgins, M. W., and Zietz, I., 1976. Preliminary interpretation of
844 aeromagnetic and aeroradioactivity maps of the Alabama Piedmont: *Geology*, v. 4, p.
845 375-381.

846 Newton, M.C., III, and Romeo, A.J., 2006, Geology of the Old Hickory heavy mineral sand
847 deposit, Dinwiddie and Sussex counties, Virginia, in Reid, Jeffrey C., editor, Proceedings
848 of the 42nd Forum on the Geology of Industrial Minerals: North Carolina Geological
849 Survey Information Circular 34, p. 464-481.

850 North American Magnetic Anomaly Group, 2002, Magnetic Anomaly Map of North America:
851 U.S. Geological Survey Special Map, http://pubs.usgs.gov/sm/mag_map/

852 Overstreet, W.C., 1967, The geologic occurrence of monazite: U.S. Geological Survey
853 Professional Paper 530, 327 p., 2 plates

854 Owens, J.P. and Gohn, G., 1985. Depositional history of the Cretaceous Series in the U.S.
855 Atlantic coastal plain: stratigraphy, paleoenvironments and tectonic controls of
856 sedimentation: *in* Poag, C.W. (Ed.), *Geologic Evolution of the United States Atlantic*
857 *Margin*. Van Nostrand Reinhold Company, New York, p. 25–86.

858 Peterson, C.D., Komar, P.D., and Scheidegger, K.F., 1986, Distribution, geometry, and origin of
859 heavy mineral placer deposits on Oregon beaches: *Journal of Sedimentary Petrology*, v.
860 56, p. 67-77.

861 Pitkin, J.A. 1968. Airborne measurements of terrestrial radioactivity as an aid to geologic
862 mapping: U.S. Geological Survey Professional Paper 516-F, v. 1-29, 42 p.

863 Prusak, D. and Mazzullo, J., 1987, Sources and provinces of late Pleistocene and Holocene sand
864 and silt on the mid-Atlantic continental shelf, *Journal of Sedimentary Petrology*, v. 57,
865 no. 2, p. 278-287

866 Ravat, D., Finn, C., Hill, P., Kucks, R., Phillips, J., Blakely, R., Bouligand, C., Sabaka, T.,
867 Elshayat, A., Aref, A., and Elawadi, E., 2009, A preliminary, full spectrum, magnetic
868 anomaly grid of the United States with improved long wavelengths for studying
869 continental dynamics--A website for distribution of data: U.S. Geological Survey Open-
870 File Report 2009-1258, 2 p.

871 Reid, A., Keeling, J., Boyd, D., Belousova, E., Hou, B., 2013. Source of zircon in world-class
872 heavy mineral placer deposits of the Cenozoic Eucla Basin, southern Australia from LA-
873 ICPMS U-Pb geochronology: *Sedimentary Geology*, v. 286-287, p. 1-19.

874 Roy, P.S., 1999, Heavy mineral beach placers in southeastern Australia: Their nature and
875 genesis: *Economic Geology*, V. 94, p. 567-588.

876 Secor, Jr., D.T., Snoke, A.W., and Dallmeyer, R.D., 1986, Character of the Alleghanian orogeny
877 in the southern Appalachians: Part III. Regional tectonic relations: *Geological Society of*
878 *America Bulletin*, v. 97, p. 1345-1353.

879 Shah, A.K. and Harris, M.S., 2012, Shipboard magnetic field data trace magnetic sources in
880 marine sediments: Geophysical studies of the Stono and North Edisto Inlets near
881 Charleston, South Carolina: U.S. Geological Survey Open-File Report 2012-1112.

882 Shah, A.K., Vogt, P., Rosenbaum, J., Newell, W., Cronin T., Willard, D., Hagen, R., Brozena, J.,
883 and Hofstra, A., 2012, Shipboard magnetic field "noise" reveals shallow heavy mineral
884 sediment concentrations in Chesapeake Bay: *Marine Geology*, v. 303-306, p. 26-41.

885 Siddiquie, H.N., Gujar, A.R., Hashimi, N.H., and Valsangkar, A.B., 1984, Superficial mineral
886 resources of the Indian Ocean, *Deep Sea Research Part A: Oceanographic Research*
887 *Papers*, v. 31, p. 763-812.

888 Singh, H.N., Shanker, V.N., Neelakandan, V.N., and Singh, V.P., 2007, Distribution patterns of
889 natural radioactivity and delineation of anomalous radioactive zones using in situ
890 radiation observations in Southern Tamil Nadu, India, *Journal of Hazardous Materials*, v.
891 141, p. 264-272.

892 Sircombe, K.N., and Freeman, M.J., 1999, Provenance of detrital zircons on the Western
893 Australia coastline—Implications for the geologic history of the Perth basin and
894 denudation of the Yilgarn craton: *Geology*, v. 27., no. 10, p. 879-882.

895 Smith, S.M., 1997. National Geochemical Database: reformatted data from the National Uranium
896 Resource Evaluation (NURE) Hydrogeochemical and Stream Sediment Reconnaissance
897 (HSSR) Program, Version 1.40 (2006): U.S. Geological Survey Open-File Report 97–
898 492. WWW release only, URL: <http://pubs.usgs.gov/of/1997/ofr-97-0492/index.html>.

899 Staatz, M.H., Armbrustmacher, T.J., Olson, J.C., Brownfield, I.K., Brock, M.R., Lemons, J.F.,
900 and Clingan, B.V., 1979, Principal thorium resources in the United States: U.S.
901 Geological Survey Circular 805, 42 p.

902 Staatz, M.H., Hall, R.B., Macke, D.L., Armbrustmacher, T.J., and Brownfield, I.K., 1980,
903 Thorium resources of selected regions in the United States: U.S. Geological Survey
904 Circular 824, 32 p.

905 Staff, Bureau of Mines, 1987, An economic reconnaissance of selected heavy mineral placer
906 deposits in the U.S. Exclusive Economic Zone: Bureau of Mines Open File Report 4-87,
907 130 p.

908 Tse, P.-K., 2011, China's rare-earth industry: U.S. Geological Survey Open-File Report 2011-
909 1042, 11 p.

910 Van Gosen, B.S., Fey, D.L., Shah, A.K., Verplanck, P.L., and Hoefen, T.M., 2014, Deposit
911 model for heavy-mineral sands in coastal environments: U.S. Geological Survey
912 Scientific Investigations Report 2010-5070-L, 51 p.,
913 <http://dx.doi.org/10.3133/sir20105070L>.

914 Watson, T.L. and Hess, F.L., 1913, Zirconiferous sandstone near Ashland, Virginia: *in* Watson,
915 T.L., Hess, F.L. and Stose, G.W., eds., Biennial Report on the Mineral Production of
916 Virginia During the Calendar Years 1911 and 1912: With Chapters on Zirconiferous
917 Sandstone Near Ashland, Virginia: Charlottesville, Virginia, University of Virginia,
918 Report No. 8, 76 p.

919 Wynn, J.C., Grosz, A.E., and Fosczyk, V.M., 1985, Induced polarization and magnetic response of
920 titanium placer deposits in the southeastern United States: U.S. Geological Survey Open-
921 File Report 85-756, 42 p.

922
923

924 Table 1. Summary of field site survey and heavy mineral separate properties

Site	Location (latitude, longitude degrees)	Max field eTh (ppm)	Laboratory sample eTh (ppm)	Magnetic Susceptibility ($\times 10^{-3}$ SI)	Monazite present?	Th (ppm)	La (ppm)	Lu (ppm)
Scientists Cliffs, Md.	38.51450, -76.51039	24.6	12.59	4.07	N	42.5	84.9	7.44
James River, Va.*	37.24243, -76.86176	1305.9		26		751	3002	
Aurelian Springs, N.C.	36.377, -77.745	27.7	40.09	14.34	N	200	408	6.98
Outer Banks, N.C.	35.68847, -75.48327	10.7	33.29	5.51	N	143	319	5.24
Cheraw, S.C.	34.63135, -79.92900	43.6		<0.1	Y			
Francis Marion, S.C.	33.22483, -79.48665	25.1		<0.1	Y			
Folly, S.C.	32.64340, -79.96450	826.8	154.14	2.9	Y	700	1640	13.1
Folkston, Ga.	31.041, -81.996	25.1	59.2	0.98		146	332	7.98
Cumberland Island, Ga.	30.84653, -81.42642	191.6	105.78	1.95	Y	269	686	9.37
Little Talbot Island, Fla.	30.44942, -81.40998	578.5	105.86	2.2	Y	312	801	11.4

925 *Heavy mineral separates were not available for this sample so measurements were conducted on bulk
926 sands. The heavy mineral concentration was very high, however, with a sample density of 2.9 g/cm³.

927 Table 2. Regional variations in sample heavy mineral separate properties

	Thorium content	Magnetic Susceptibility	Monazite content	Rutile content	Inferred dominant source type
VA and northern NC, away from major rivers	Low	Medium-high	Low	Low (with exceptions)	Low-medium grade metamorphic
Southern NC near the Fall Line	High	Medium, mixed	High	Medium, mixed	Mixed igneous and high-grade metamorphic
SC to GA near the Fall Line	High	Low (with exceptions)	High	High	High-grade metamorphic
Eastern AL near the Fall Line	High, mixed	High	High/mixed	Low	Mostly igneous, some mixed
Coastal SC, southeast GA, and northern FL	Mixed	Mixed	Mixed	Mixed	Mixed
TN and MS near the Fall Line	Low	Low	Low	Low	Ambiguous or mixed

928

929 **FIGURE CAPTIONS**

930 **Figure 1.** Geologic provinces of the southeastern U.S. Placer deposits containing ilmenite, rutile
931 and zircon are present throughout Coastal Plain sediments. REE-bearing monazite and xenotime
932 have also been observed in smaller amounts in various locales. Triangles represent ground
933 survey areas. Elongate, lightly shaded areas spanning the Piedmont and Blue Ridge provinces
934 represent “monazite belts” of Mertie (1979). Ages of Coastal Plain sediments were obtained
935 from combined state geologic maps available online from the U.S. Geological Survey Mineral
936 Resources On-Line Spatial Data website, <http://mrdata.usgs.gov>.

937 **Figure 2.** Left: Geologic belts of the Piedmont province (combined from Hatcher and Odum,
938 1980; Secor et al., 1986; Hibbard et al., 2002). Striped areas delineate “monazite belts” by Mertie
939 (1979). The Raleigh/Goochland, Kiokee, Inner Piedmont, and Pine Mountain belts as well as the
940 Blue Ridge province are associated with high-grade metamorphism, whereas the Charlotte,
941 Carolina slate belt and Eastern slate belt are characterized by lower-grade metamorphism. The
942 Charlotte and Carolina slate belts are marked by numerous intrusions.

943 **Figure 3.** Top: NURE radiometric equivalent thorium (eTh; ppm) superimposed over shaded
944 relief topography. Bottom: NURE radiometric K (%) over shaded relief topography. Radiometric
945 data were gridded from processed flight line data by Duval et al. (2005). Dashed line represents
946 the inland boundary of Coastal Plain sediments, also referred to as the “Fall Line” where it is
947 adjacent to the Piedmont and Blue Ridge provinces. Elevation data are from the Shuttle Radar
948 Topography Mission (SRTM).

949 **Figure 4.** NURE radiometric equivalent thorium (eTh; left) and aeromagnetic anomaly (right)
950 (Ravat et al., 2009) over the Piedmont and Blue Ridge provinces. Belts with high-grade
951 metamorphic rocks are associated with eTh highs; broad magnetic highs in these areas are

952 commonly associated with secondary magnetite. Certain intrusive bodies in lower-grade
953 metamorphic belts also exhibit local eTh highs and magnetic anomalies, especially in the
954 Charlotte and Carolina slate belts. Gray lines delineate monazite belts by Mertie (1979).

955 **Figure 5.** Thorium (upper left) and monazite (lower left) concentrations, magnetic susceptibility
956 (upper right) and rutile concentrations (lower right) measured from heavy mineral separates of
957 sand samples are indicated with colored circles. Monazite and rutile were estimated using X-ray
958 diffraction (XRD). Background image shows NURE aeroradiometric equivalent thorium (eTh).
959 Polygons show geologic belts (see Figure 2). Additional sample characteristics are shown in the
960 GSA Data Repository.

961 **Figure 6.** South Carolina airborne total count survey data (top) and NURE radiometric
962 equivalent thorium (eTh; bottom) draped over shaded relief topography. The total count data
963 were collected with a flight line spacing of 1.8 km, whereas the NURE data were spaced 3-6 km.
964 Triangles represent ground survey sites labeled in Figure 1. Piedmont features from Horton and
965 Dicken (2001).

966 **Figure 7.** Geophysical survey and grab sample measurements for Little Talbot Island, FL (A-C)
967 and Folly Beach, SC (D-E). A: Satellite image, survey path (orange lines), and grab-sample
968 thorium determined via XRF. B: Radiometric equivalent thorium (eTh) obtained via continuous
969 surveys. C. Magnetic residual anomaly. D. Radiometric eTh obtained via 120-second assays
970 (white x's) and grab-sample thorium estimated via XRF (boxes). E. Magnetic anomaly and grab-
971 sample magnetic susceptibility (boxes).

972 **Figure 8.** Radiometric and magnetic anomaly data collected along single profiles on the eastern
973 shores of Cumberland Island, GA (top profiles) and the Outer Banks, NC (bottom profiles). XRF
974 measurements were also conducted on grab samples; gray symbols show sample Th. For the

975 Cumberland Island magnetic anomaly, the gray line shows the residual anomaly, and the black
976 line shows the same anomaly with a linear trend removed. Note differences in y-axis scales.

977 **Figure 9.** Geophysical drill hole data in Aurelian Springs, NC. White circles show drill collars,
978 colored squares show heavy mineral concentrations for 5-meter intervals. Pink circles show
979 USGS auger holes AS-A1 (west) and AS-A2 (east). Background image shows elevation. Top:
980 Radiometric eTh from 2-minute assays (colored swath). Drill hole data courtesy of Iluka, Inc.
981 (colored boxes). Bottom: magnetic anomaly (colored swath). Inset shows location, colors as in
982 Figure 1; triangle marks the survey site location.

983 **Figure 10.** Downhole measurements made on bulk sands derived from auger holes in Aurelian
984 Springs, NC (AS; see Figure 7 for locations) and Cheraw, SC (CH; see also GSA data
985 repository). “A1” auger holes are located within radiometric eTh highs; “A2” auger holes were
986 in radiometric eTh lows. Th and Ti were measured by inductively coupled plasma–atomic
987 emission spectrometry–mass spectrometry (ICP-AES-MS); magnetic susceptibility measured
988 using a ZH Instruments SM-30.

989 **Figure 11.** Geophysical data and drill hole data near Folkston, Georgia. Circles show drill
990 collars, colored squares show heavy mineral concentrations for 2.5-foot intervals. Yellow dashed
991 line shows an approximate boundary of the heavy mineral resource. Background image shows
992 satellite imagery. Top: Radiometric equivalent thorium (eTh; colored swath) and heavy mineral
993 concentrations (HM; colored boxes). Middle: magnetic anomaly (colored swath) and heavy
994 mineral concentrations (HM; colored boxes). Bottom: Location within a series of Pleistocene
995 ridges. Triangle marks the survey site. Drill hole data provided courtesy of Southern Ionics, Inc.

996 **Figure 12.** Top: Radiometric equivalent thorium (eTh; background) shows high values in parts
997 of the Atlantic Coastal Plain inferred to contain elevated monazite and xenotime (red outlines);

998 grayed areas represent carbonate rocks (also associated with eTh highs). Black lines delineate
999 belts of the Piedmont and Blue Ridge provinces. Bottom: Belts of the Piedmont and Blue Ridge
1000 have been colored according to rock type. Heavy mineral sands in the Atlantic Coastal Plain
1001 show regional compositional variations that suggest they were derived from specific rock types.
1002 These rock types correspond to Piedmont or Blue Ridge units adjacent to Atlantic Coastal Plain
1003 sediments. Dashed shapes delineate areas believed to contain elevated monazite and xenotime
1004 concentrations.

1005

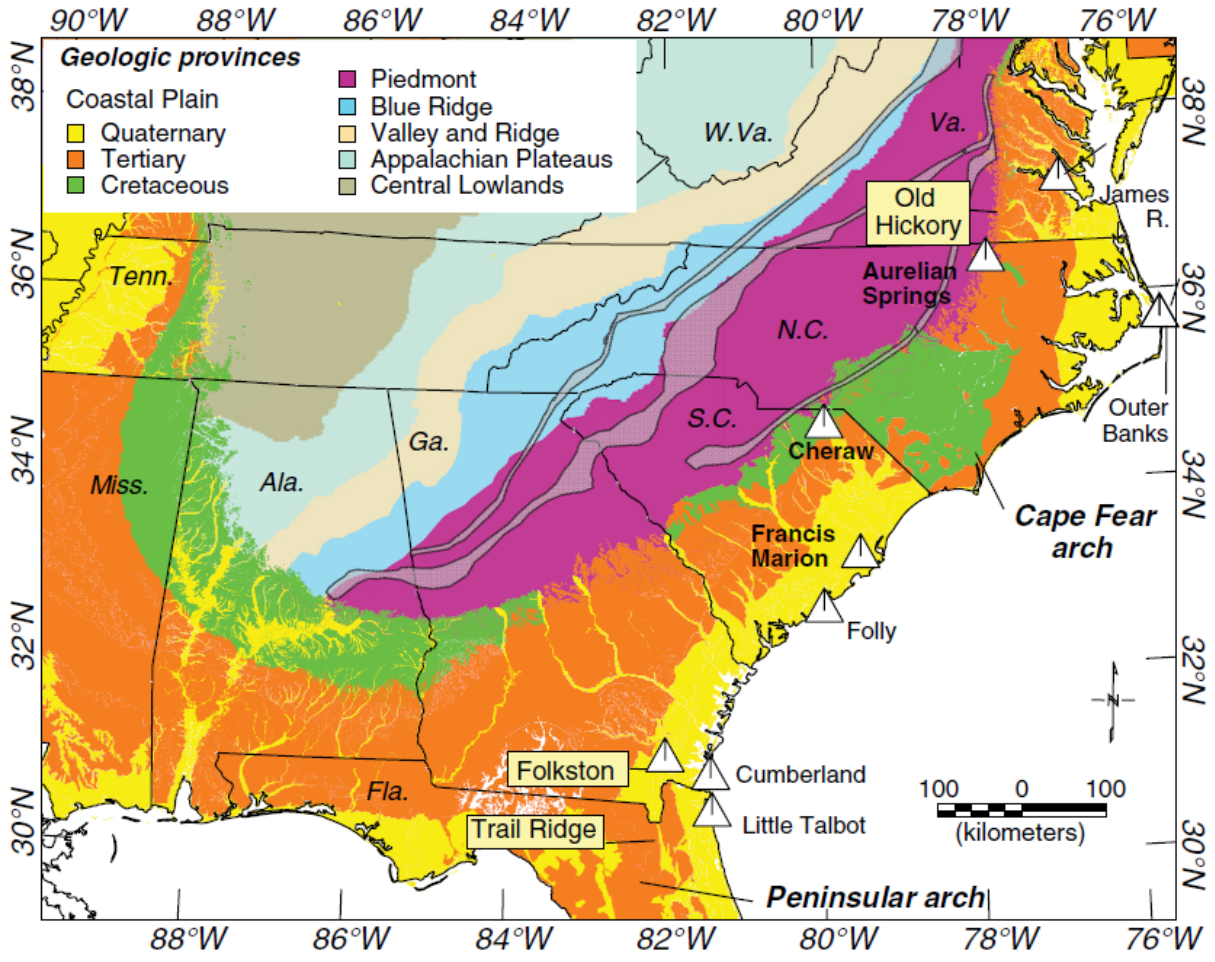
1006 ¹GSA Data Repository item 201Xxxx, Comparison of the RS-125 to the Gamma Surveyor, is
1007 available online at www.geosociety.org/pubs/ft20XX.htm, or on request from
1008 editing@geosociety.org or Documents Secretary, GSA, P.O. Box 9140, Boulder, CO 80301,
1009 USA.

1010 ²GSA Data Repository item 201Xxxx, Additional sample properties, is available online at
1011 www.geosociety.org/pubs/ft20XX.htm, or on request from editing@geosociety.org or
1012 Documents Secretary, GSA, P.O. Box 9140, Boulder, CO 80301, USA.

1013 ³GSA Data Repository item 201Xxxx, Additional grid surveys for Aurelian Springs, N.C. and
1014 Cheraw, S.C., is available online at www.geosociety.org/pubs/ft20XX.htm, or on request from
1015 editing@geosociety.org or Documents Secretary, GSA, P.O. Box 9140, Boulder, CO 80301,
1016 USA.

1017

1018

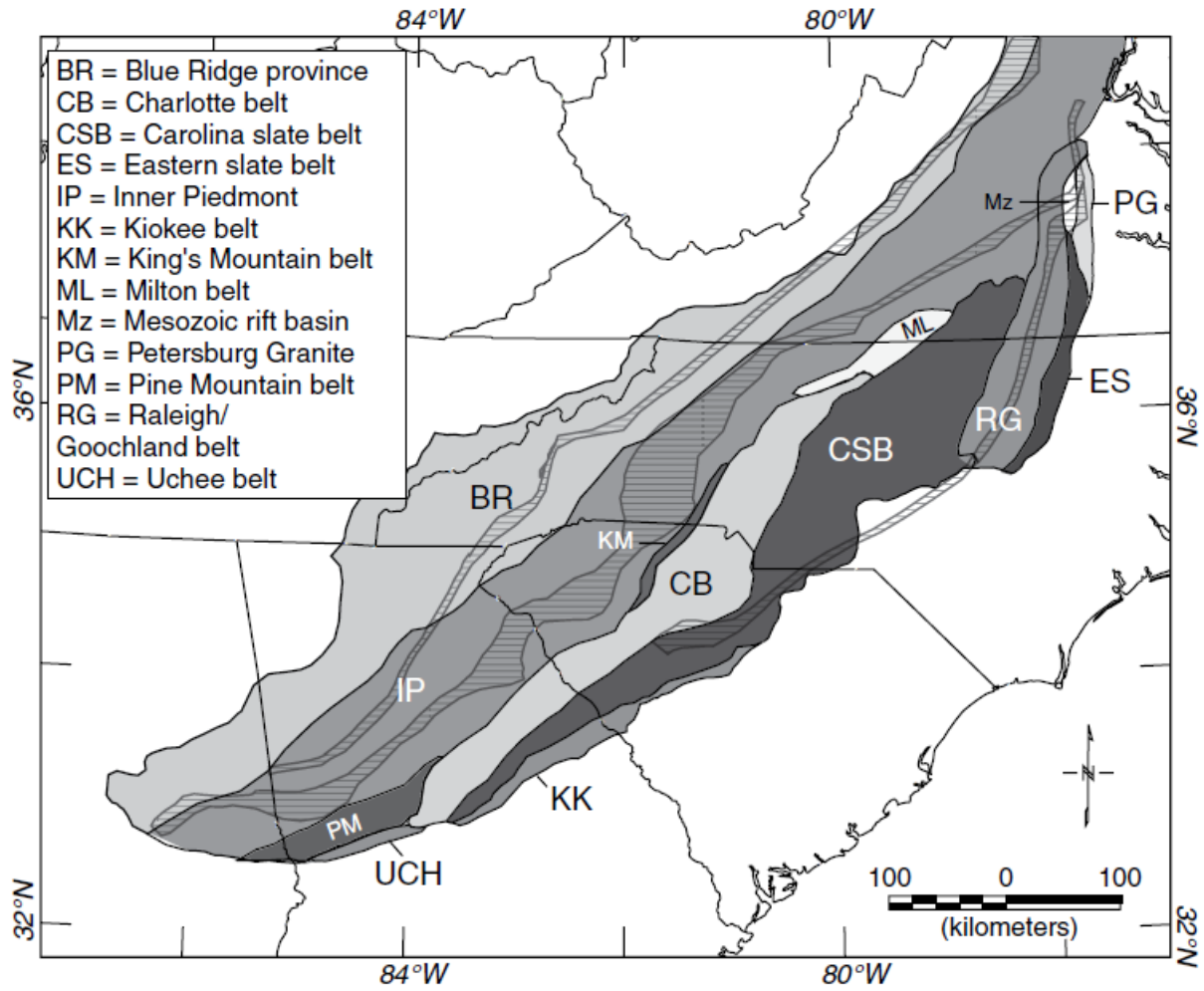


1019

1020

1021 Figure 1

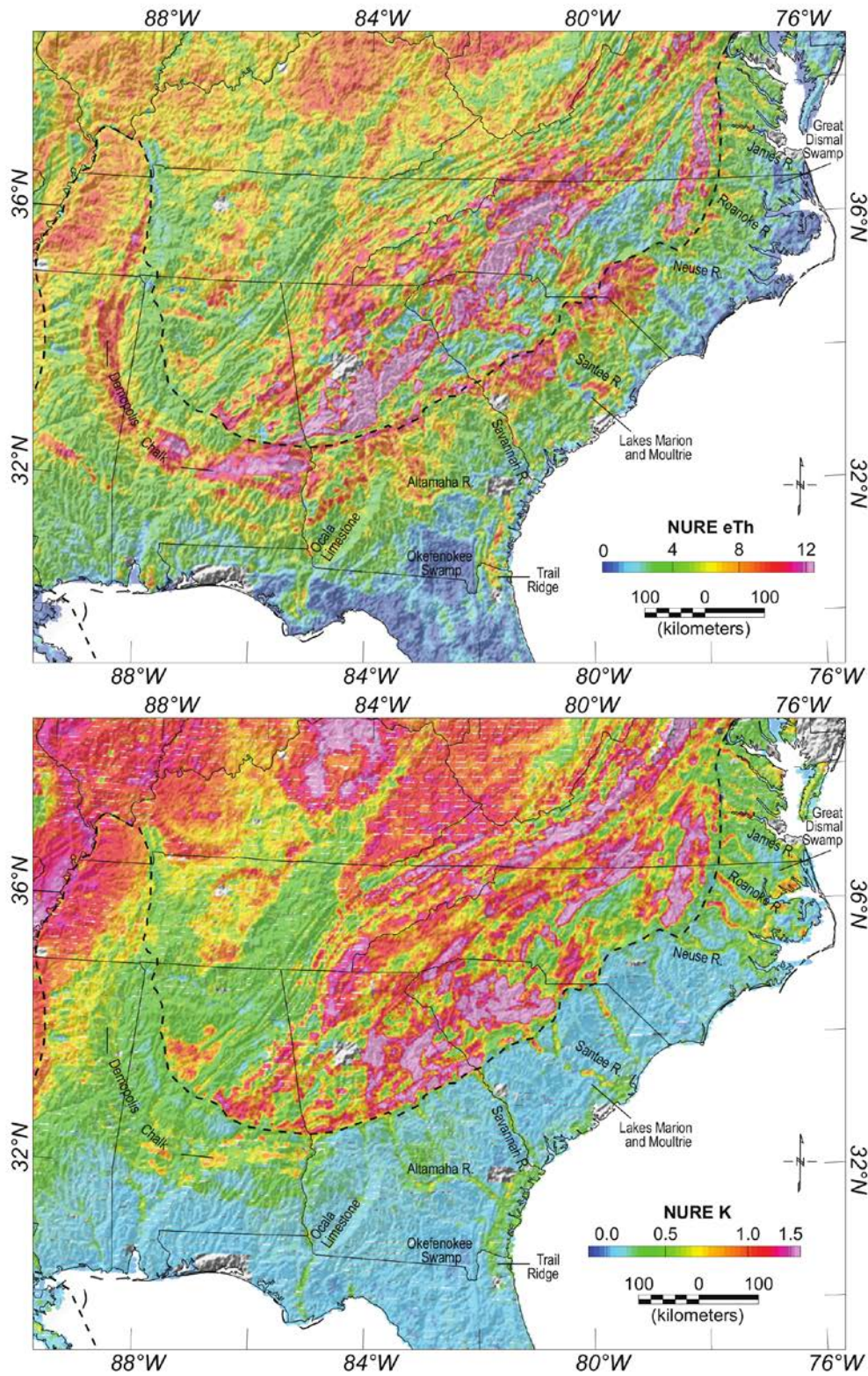
1022



1023

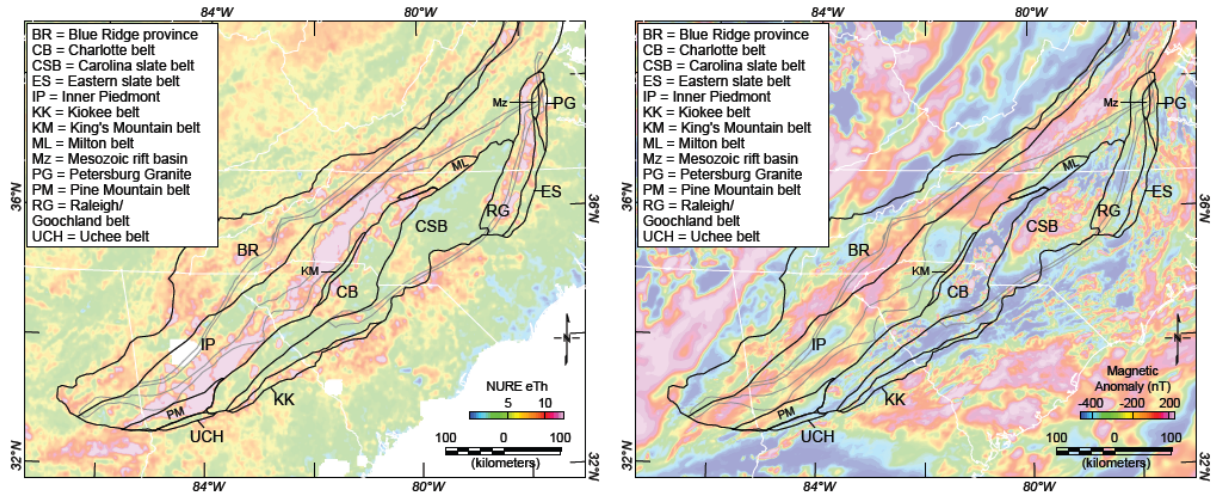
1024 Figure 2

1025



1026

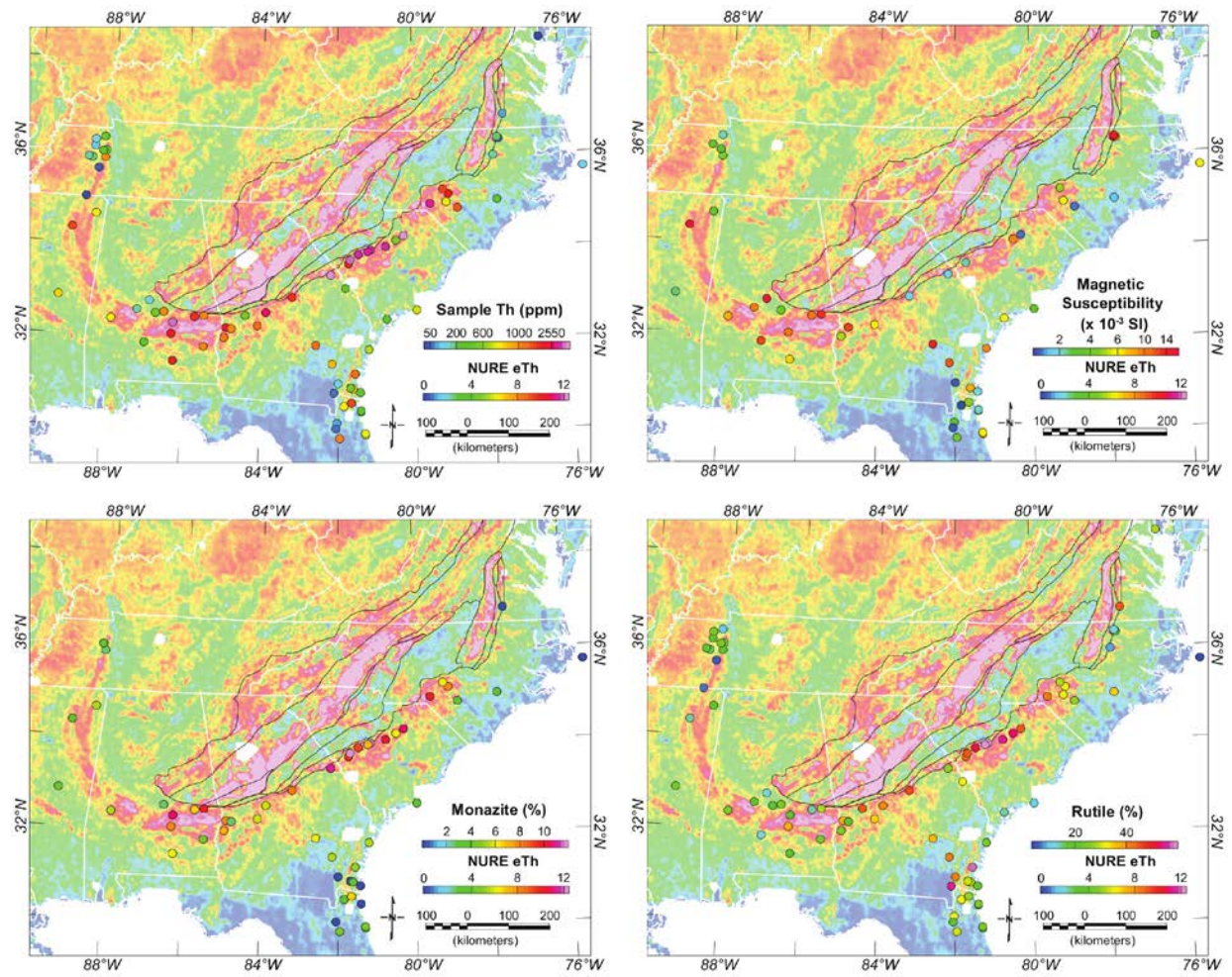
1027 Figure 3.



1028

1029 Figure 4

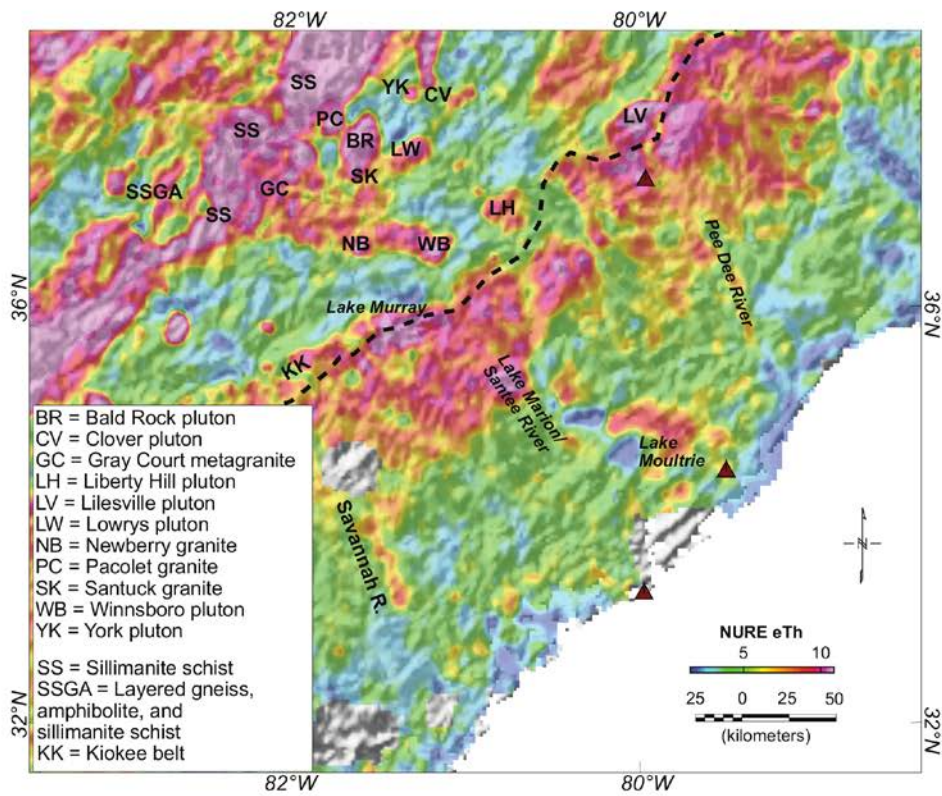
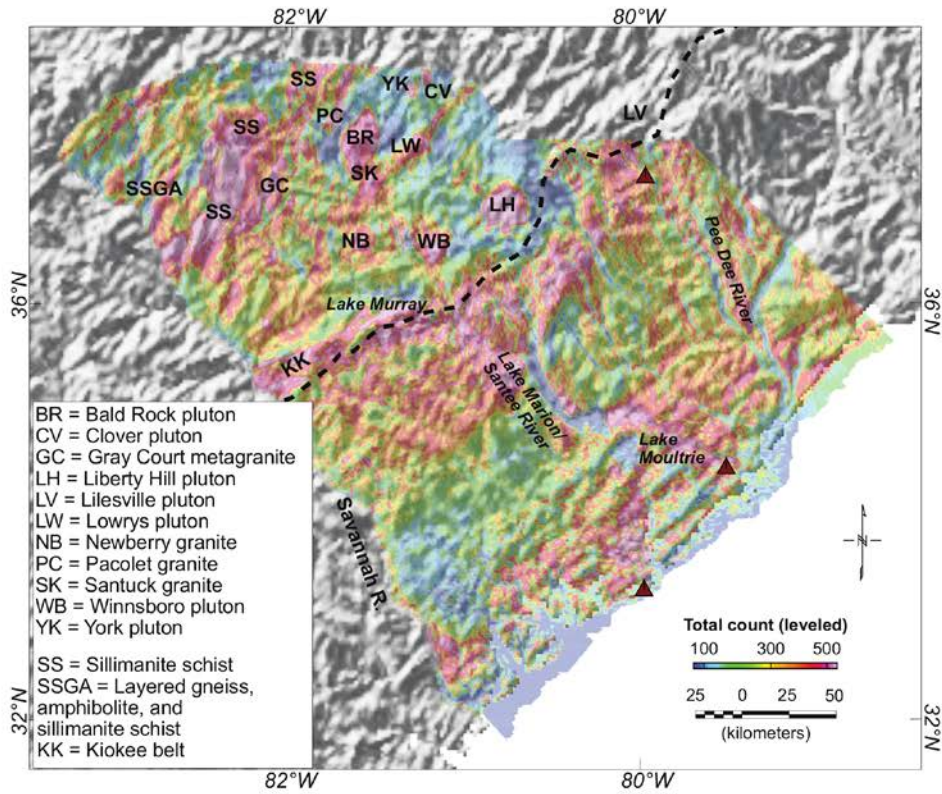
1030



1031

1032 Figure 5

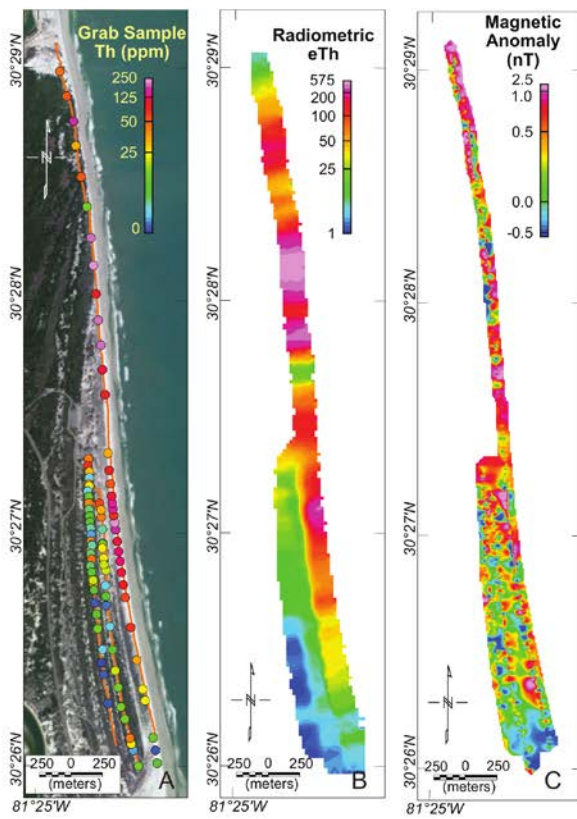
1033



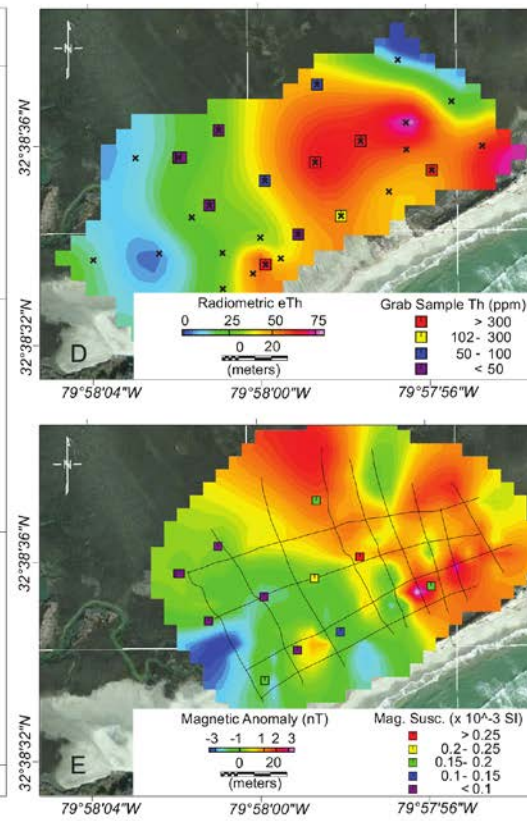
1034

1035 Figure 6

Little Talbot Island, Fla.



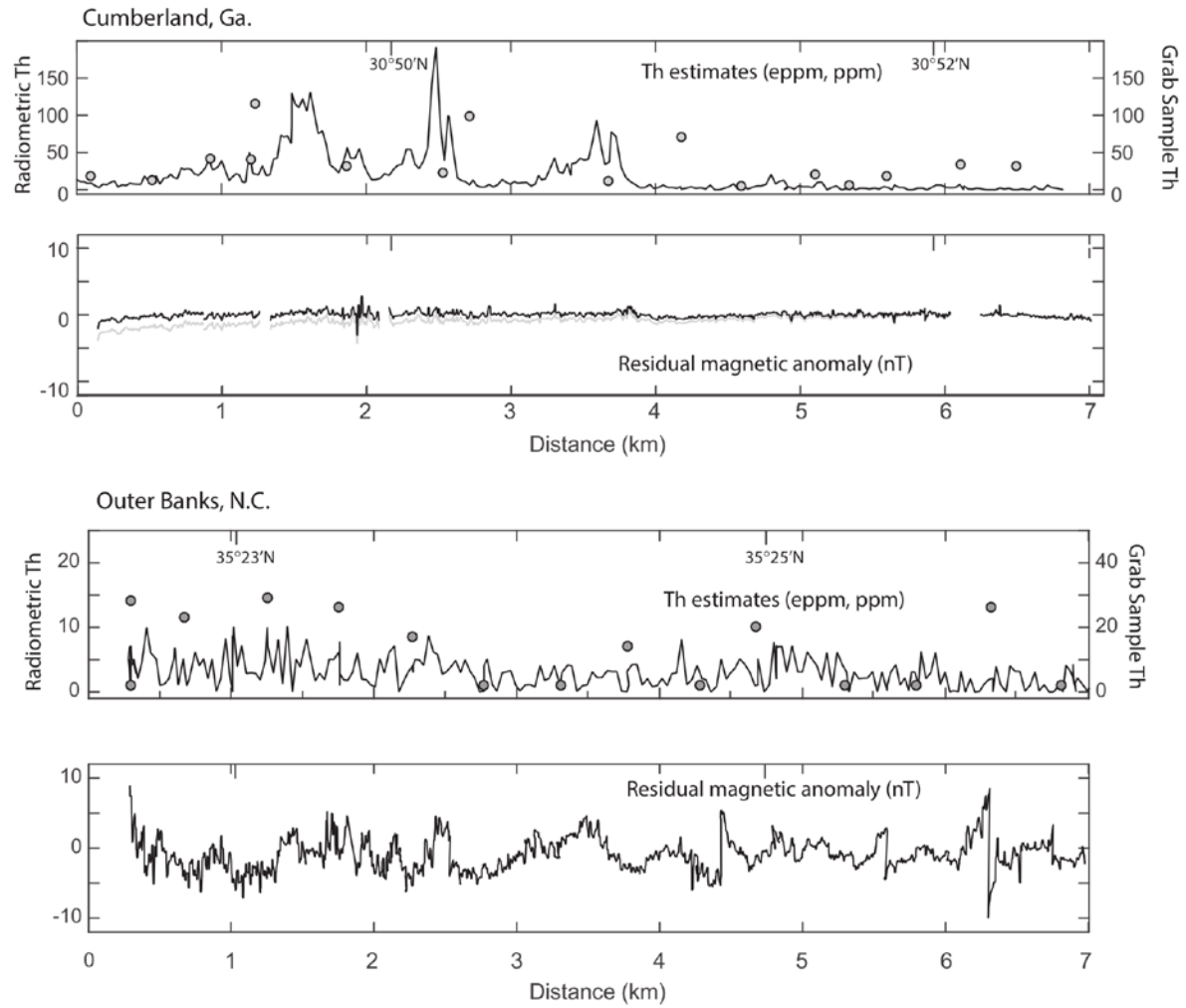
Folly Beach, S.C.



1036

1037 Figure 7

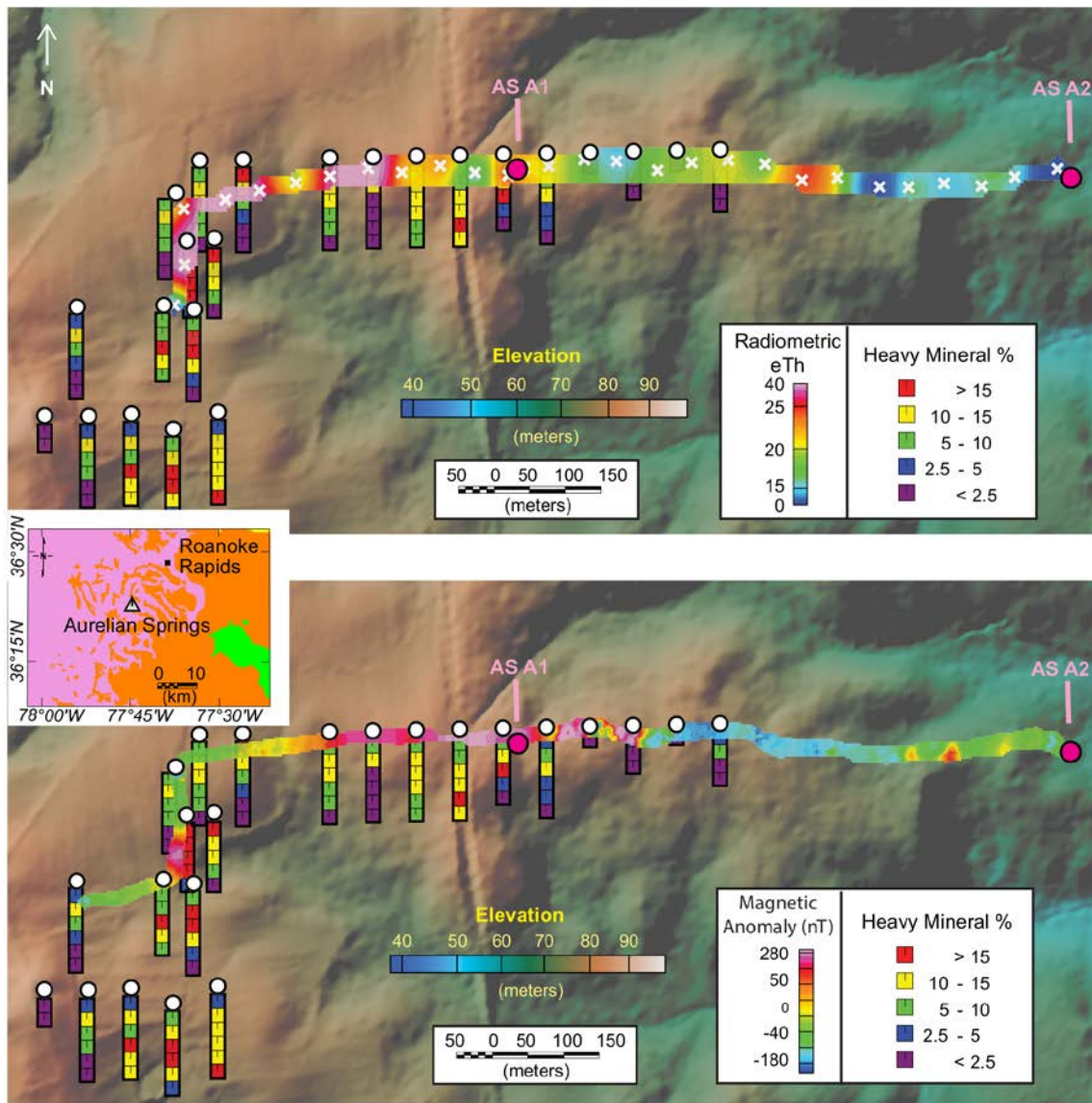
1038



1039

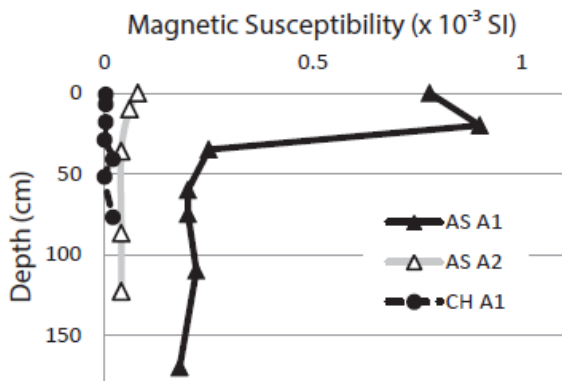
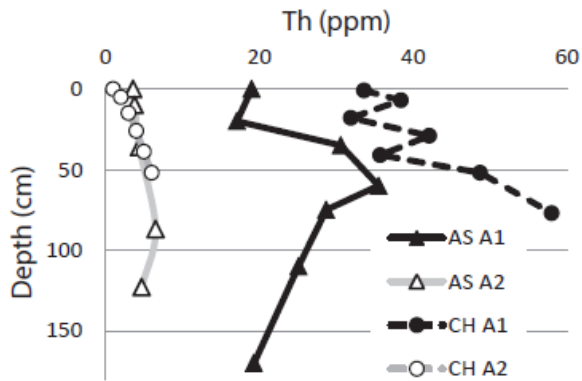
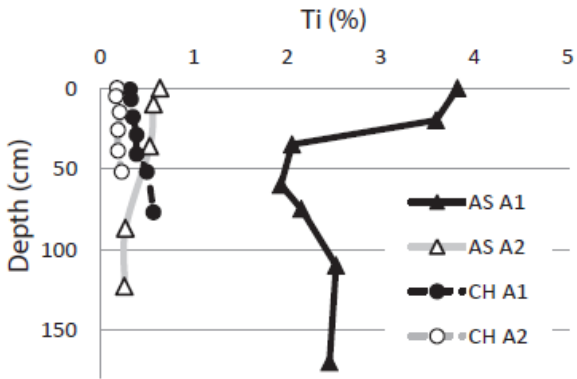
1040 Figure 8

1041



1042

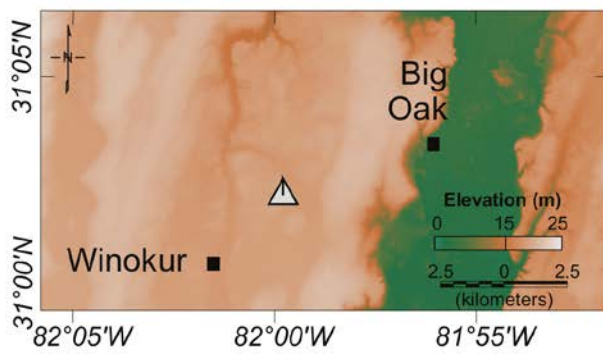
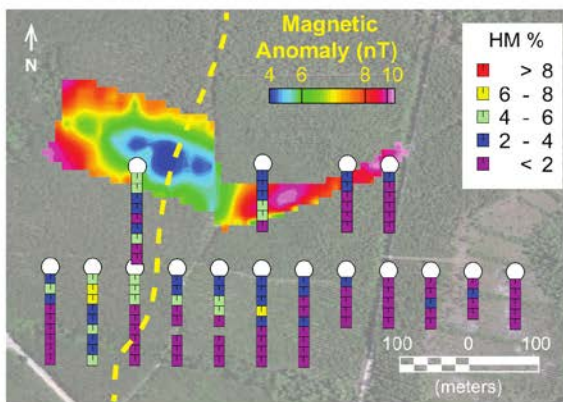
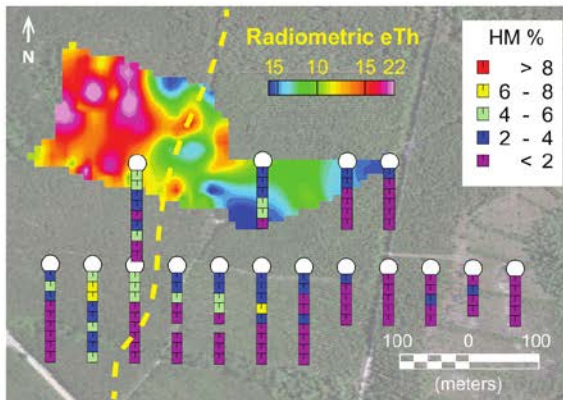
1043 Figure 9



1044

1045 Figure 10

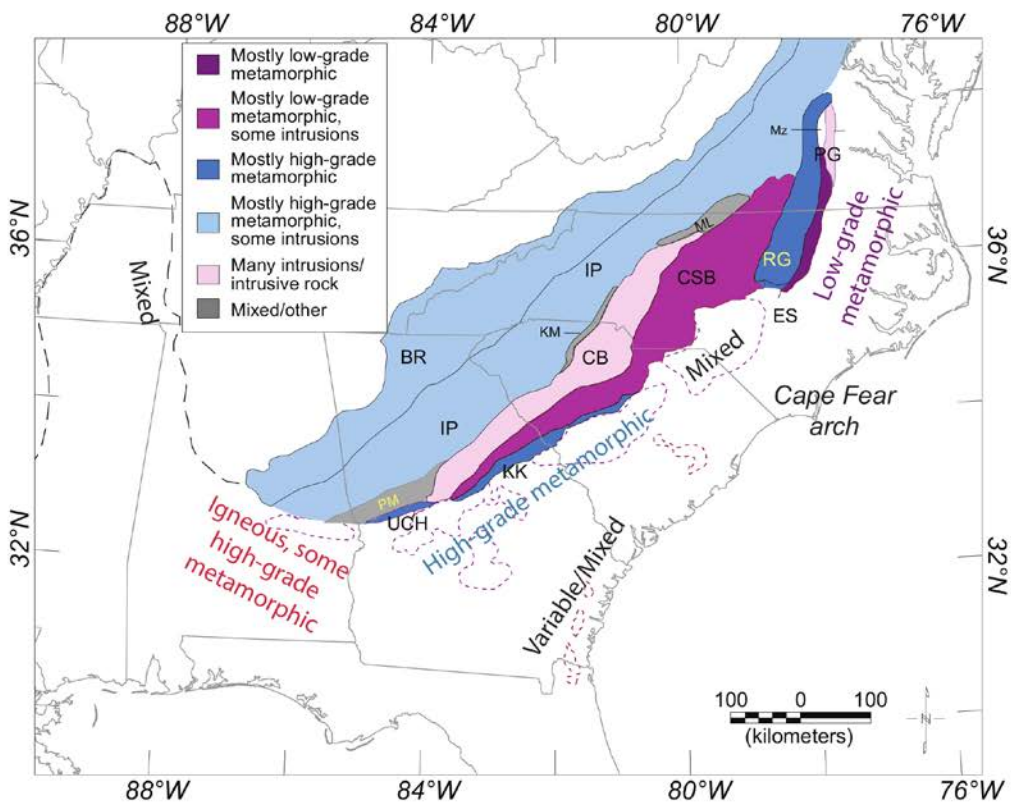
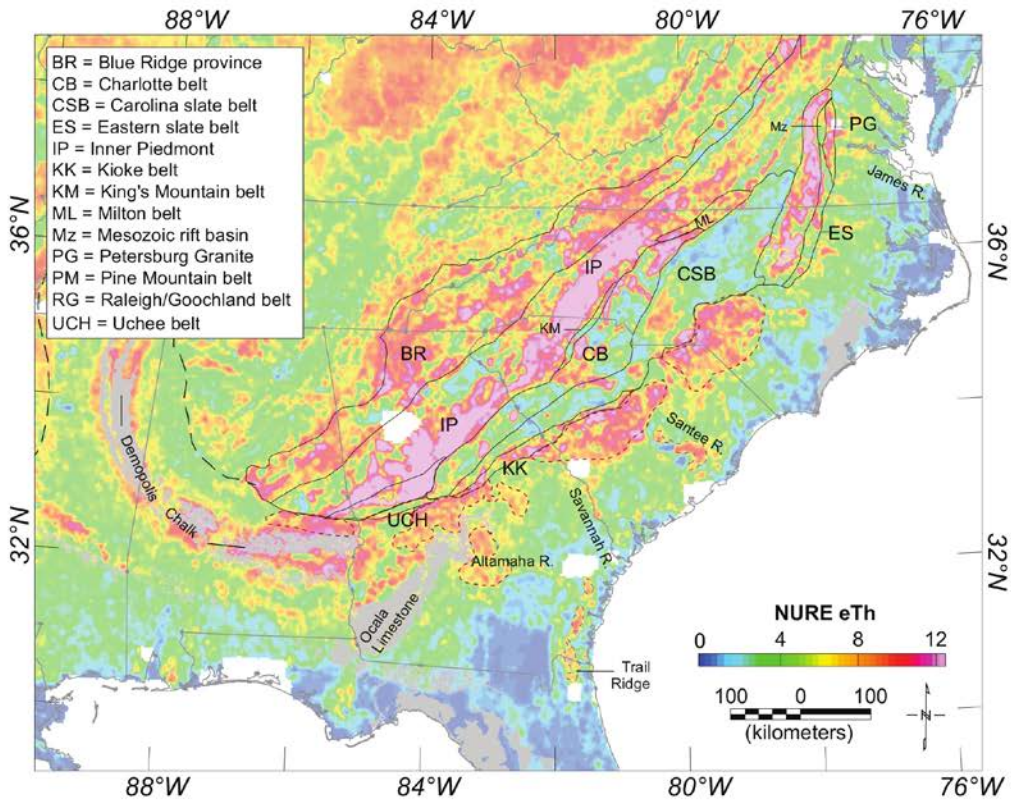
1046



1047

1048 Figure 11

1049



1050

1051 Figure 12